Voltage-Gated Sodium Channels and their Role in Prostate Cancer

by

Madeline Angus

B.Sc., Simon Fraser University, 2016

Thesis Submitted in Partial Fulfillment of the
Requirements for the Degree of
Master of Science

in the
Department of Biomedical Physiology and Kinesiology
Faculty of Science

SIMON FRASER UNIVERSITY
Fall 2019

Approval

Name:	**Madeline Angus**
Degree:	**Master of Science**
Title:	**Voltage-Gated Sodium Channels and their Role in Prostate Cancer**
Examining Committee:	**Chair:** Sam Doesburg Associate Professor
	Peter Ruben Senior Supervisor Professor
	Sharon Gorski Supervisor Professor Department of Molecular Biology and Biochemistry
	Tim Beischlag Supervisor Professor Department of Health Science
	Nadine Wicks Internal Examiner Lecturer
Date Defended/Approved:	December 9th 2019

Abstract

Voltage-gated sodium channels (VGSC) increase invasiveness and metastatic potential in prostate cancer and may be a novel drug target for castration resistant prostate cancer. VGSC isoforms expressed in prostate cancer differ depending on cell type, and laboratory growing conditions Immunocytochemistry experiments suggest that VGSC localize in invadopodia, structures required for invasiveness of cancer cells. VGSC significantly colocalize with vimentin, a marker of invadopodia ($p<0.0001$) and display polarized expression patterns on the cell membrane. Functional invasion experiments using a variety of VGSC blockers such as tetrodotoxin, lidocaine, and cannabidiol demonstrate that VGSC inhibition significantly reduces cancer invasiveness ($p<0.0001$). These results suggest that VGSC plays a functional role in invadopodia and VGSC inhibition reduces invasiveness and metastatic potential in prostate cancer.

Keywords: Voltage-gated sodium channels; cancer; immunocytochemistry; invasion assays; patch clamping, cell invasion

Acknowledgments

I would like to thank Dr. Peter Ruben for believing in me and inspiring me to take a post secondary degree. He took on a master's student with no prior research experience and with nothing but an idea that had not been done before. He allowed me to design my own project, which was very much outside of the ordinary for an electrophysiology lab and has supported me for the entirety of my education journey. I would like to thank Dr. Colin Peters for helping me to see the beauty and value of research for the sake of research, and for supporting me and encouraging me through my successes and failures in the lab. I would like to thank Maxine Owers and Mariam Aziz Hanna for being three wonderful undergraduate students to work with. I would finally like to thank the Ruben lab and the rest of the Molecular Cardiac Research Group for making the last couple of years an enjoyable journey.

I would like to thank Dr. Nader Al Nakouzi for providing me with data for the immunohistochemistry experiments and his interest in my research project. I would also like to thank Robert Payer and the members of Dr.Tim Beischlag's lab for teaching me how to do western blots, providing me with the finished plasmids and reagents to generate the CRISPR knockout lines. I would also like to further thank Robert Payer for providing me with the western blots of different voltage-gated sodium channel isoforms.

Table of Contents

List of Tables

List of Figures

Copyright

Chapter 1.

Introduction

1.1. Prostate Cancer

Cancer kills 8.2 million people every year, with a 38.82 percent probability of a person developing cancer in their lifetime according to Cancer Statistics (data from the United States) [1] The most common types of cancer include skin cancer (276,250 cases expected annually in the United States), lung cancer (226,160 cases expected annually), prostate cancer (241,740 cases expected annually), and breast cancer (226,870 cases expected annually). [1] Cancer is a disease of rapid and uncontrolled cell proliferation either due to excessive cell division, lack of regulated apoptosis or a combination of the two. [2] Development of cancer involves the accumulation of DNA mutations over time and risk increases with exposure to carcinogens or with age. [2] In particular, DNA mutations in proto-oncogenes, proteins involved in stimulating growth and cell division pathways, and in tumor suppressors, proteins that regulate the cell cycle and stimulate apoptosis can promote the development of cancer. [2]

Approximately 1 in 6 men in the United States will be diagnosed with prostate cancer during their lifetime. [3] Prostate cancer is the second leading cause of cancer-related deaths in males. [3] An estimated number of 28,170 men die of prostate cancer each year in the United States. [1] Prostate specific antigen (PSA) screening and digital rectal exams can help with early detection and if caught early, prostate cancer has nearly a 100 percent 5 year survival rate. [4]

If prostate cancer is detected before metastasis has occurred, treatment typically consists of surgery to partially or totally remove the prostate gland, and radiation therapy. [5] If the prostate tumor is very large or has already metastasized, hormone therapy may be advised.[6] Hormone therapy consists of chemical castration, or removal of androgens in the body through use of drugs. [6,7] Since the prostate is a testosterone sensitive tissue, with prostate cells requiring a supply of testosterone in order to grow and divide, removal of testosterone in the body causes prostate tumors to shrink or grow more slowly. [5] In some cases, prostate cancer cells become unresponsive to hormonal

treatment and can become highly invasive once again. Prostate cancer that has become resistant to treatment is called castration resistant prostate cancer.[5] 10-20% of prostate cancer patients develop castration resistant prostate cancer within 5 years of the initial cancer diagnosis.[8] Once castration resistant prostate cancer develops predicted survival drops to 1-2 years.[1] The final stage of prostate cancer is neuroendocrine prostate cancer which occurs in 20-30% of patients with castration resistant prostate cancer.[9] In neuroendocrine prostate cancer cells become resistant to most forms of treatment and little can be done for patients other than offer palliative care.[10]

Neuroendocrine prostate cancer is lethal with a median survival of < 1 year after detection.[1] Neuroendocrine prostate cancer is characterised by loss of androgen receptor (AR) expression making it resistant to androgen deprivation therapy.[11,12] Neuroendocrine prostate cancer cells cease to express PSA and begin to express markers typical of neurons and endocrine cells.[11,12] Neuroendocrine cells also begin to develop highly invasive axon-like projections that are quick to invade into surrounding structures. Due to limited treatment options it is imperative to identify novel therapeutic targets that may function to reduce metastasis in castration resistant and neuroendocrine prostate cancer.

1.2. Voltage-gated sodium channels as a novel therapeutic target in late stage prostate cancer

A novel drug target for late stage prostate cancer may be presented in the form of voltage-gated sodium channels (VGSC), ion channels that are expressed in cancer and may play a functional role in invasiveness. VGSC are found in cancers of the breast,[2] colon, lung,[3] prostate,[4] cervix,[5] ovary,[6] as well as in lymphomas[6] and melanomas.[6] VGSC are mostly known for their function in the generation and propagation of action potentials in electrically excitable cells such as neurons and muscle fibers. VGSC are strongly upregulated and conserved across many different types of cancer[13,14] suggesting that they impart some advantage or survivability to cancer cells.

VGSC expression increases cell motility and invasiveness in cancer cells. [13–18] Expression of VGSC has been associated with increased movement, contact independence, and metastatic potential in various types of cancer.

Although exact mechanisms in cancer cells remain unknown, VGSC are found in several non-cancerous, non excitable cell types such as microglial cells[19,20] and macrophages[21,22] where they are thought to play a role in assisting cells to degrade the extracellular matrix (ECM) and migrate rapidly through tissue microenvironments. Deducing the mechanism by which VGSC act to increase invasiveness in cancer is key to developing a novel VGSC specific approach for castration resistant prostate cancer treatment.

1.3. Hypothesis

My overall hypothesis for this project is that voltage-gated sodium channels increase invasiveness and metastatic potential in prostate cancer by a functional role in invadopodia.

1.4. Specific Aims

1.4.1. Aim 1: Determine which VGSC isoforms are expressed in prostate cancer cells

My first aim was to determine which VGSC isoforms appear in prostate cancer cells. I did this by first characterizing the endogenously expressed VGSC using patch clamp recordings to test the hypothesis that the sodium channels reported in the literature behave as traditional voltage-gated channels. Secondly, I explored differences in isoform expression by using qPCR for PC3 and LNCaP cells.

1.4.2. Aim 2: Determine if VGSC localize in the leading edge of the cell

My second aim was to test the hypothesis that VGSC localize in invadopodia. To test this idea, I conducted a series of immunocytochemistry experiments to visualize and quantify VGSC localization. I imaged prostate cancer cells and stained for VGSC and the actin cytoskeleton, and conducted a colocalization analysis of VGSC and vimentin, a marker of invadopodia. This allowed me to visualize VGSC localization and determine if VGSC expression is found exclusively in the invading edge of the cell.

1.4.3. Aim 3: Test the hypothesis that VGSC inhibition reduces invasiveness in prostate cancer cells

My third and final aim was to determine the potential of a VGSC focused therapeutic approach on reducing prostate cancer cell invasiveness conducting a series of drug experiments. I tested the hypothesis that VGSC inhibition reduces cell invasion by conducting invasion assays using a variety of VGSC inhibitors. I used Matrigel coated chambers that are specifically formulated to test cancer cell invasion. This allowed me to

determine the effects of VGSC inhibition on cell invasion and discuss the potential of VGSC as a novel therapeutic target for prostate cancer.

1.5. Significance

There are limited treatment options available for patients with late stage prostate cancer. VGSC appears to be a promising therapeutic target and exploring the effectiveness of inhibiting this channel is necessary as a first step toward developing a potential VGSC-specific approach to treating prostate (and, potentially other forms of) cancer.

Chapter 2.

Background: Literature Review

2.1. Voltage-gated sodium channel structure and function

2.1.1. Function

Voltage-gated sodium channels (VGSC) conduct sodium ions into the cell when open which depolarizes the cell membrane.[23,24] This feature is most commonly exhibited in the action potential, where VGSC are responsible for the generation of the upstroke or depolarization phase. The action potential is exhibited in electrically excitable tissues such as the central and peripheral nervous system such as neurons in the brain and spinal cord as well as cardiac and skeletal muscle. [22] VGSC activate in response to a slight depolarization, open, and conduct sodium ions into the cell from the extracellular matrix. [22] This channel opening is shortly followed by inactivation, which quickly ceases the entry of sodium ions. VGSC mediated depolarization often activates other voltage-gated ion channels to required to complete the action potential. In this fashion, VGSC activity is critical for the transmission of neural and muscular impulses. The general features of activation, channel opening and inactivation are common to channel function for all of the VGSC isoforms.

2.1.2. Structure

There are different subtypes of VGSC that are differentially expressed throughout the body. Nav1.1, Nav1.2, Nav1.3, Nav1.6, Nav1.7, Nav1.8 and Nav1.9 are expressed in nervous tissue whereas Nav1.5 and Nav1.4 are expressed in skeletal and cardiac muscle respectively. The VGSC family consists of nine different α-subunits (Nav1.1–Nav1.9) and four β-subunits (Navβ1–Navβ4). Each sodium channel is made up of an α subunit forming the channel pore and two auxillary β subunits. (Reference Figure 1-2)

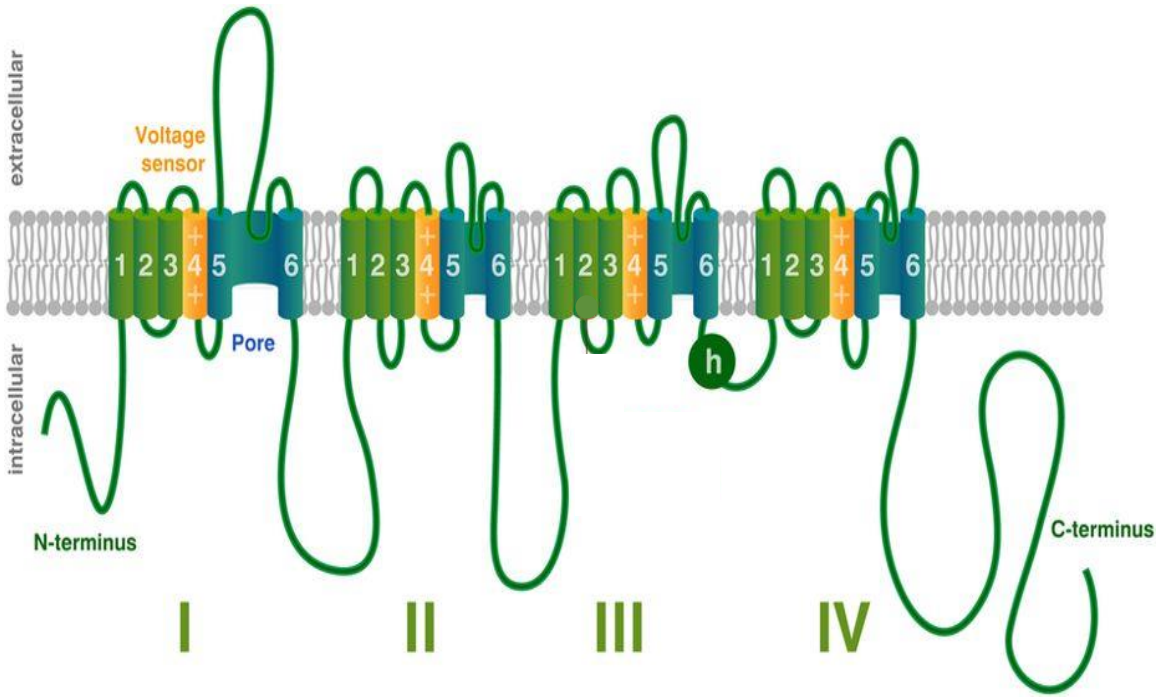

Figure 1. Structure of a generic α subunit of a voltage-gated sodium channel.
Modified from Peters, Rosch, et al. Open Access License CC BY 4.0 [25]

2.1.3. The α subunit

The α subunit consists of four domains (I, II, III and IV) each with six transmembrane segments, S1-S6.[24] The S1-S4 segments serve as the voltage sensor, whereas segments S5 and S6 line the inside of the channel pore.[24] The linker between domains III and IV is the fast inactivation gate, which operates in a 'hinged lid' fashion to inactivate the channel shortly after opening. [26]

S4 movement is responsible for channel pore opening and causes activation of the channel. In response to membrane depolarization an S4 segment from each of the four domains moves outward. The S4 segments contain regularly spaced arginine and lysine residues which are positively charged. [27] When the membrane becomes depolarized the intracellular milieu becomes more positive. This change in membrane potential repels the positively charged S4 segments outwards, which opens the channel.

The selectivity filter of the channel is formed by residues within segments S5 and S6. The selectivity filter is designed in such a way that it can distinguish between ions of similar size and charge. The innermost ring of the selectivity filter is made up of four

residues, aspartate, glutamate, lysine and alanine, one from each domain. [28] Sodium is drawn to the negatively charged glutamate residue and is subsequently conducted through the channel. Potassium forms a weaker interaction with the glutamate than sodium, and is repelled more strongly by the positive lysine residue. [28] The size of the pore is as also a contributing factor to the higher affinity forsodium. Potassium requires a larger pore because potassium can't shed its hydration shell. Sodium channels have smaller pore openings, so potassium is less likely to permeate. In this fashion the selectivity filter allows for a much higher affinity for sodium than other cations.

2.1.4. Channel opening

There are two gates in the sodium channel, an activation gate and an inactivation gate. The activation gate is closed at rest, rapidly opens in response to depolarization, and rapidly closes in response to repolarization. [29] In the activated state the S4 segments move outwards, repelled by the positive intracellular milieu. Movement of the S4 segment causes a conformational shift in the channel that causes it to open. The S4 helix is tied to the S5 helix so when the S4 moves it tugs on the S5, which causes the channel to open.[30] When the channel is open, the pore must fill with water before it can conduct any ions. When the pore becomes filled with water sodium ions are free to be conducted into the cell.

2.1.5. Fast inactivation

There are two types of inactivation, slow and fast. While fast inactivation occurs during the time frame of miliseconds, slow inactivation takes seconds, or even minutes to occur. [31]Slow inactivation takes longer to occur than fast inactivation and takes the channels longer to recover from.

The inactivation gate follows different voltage dependence and kinetics from those of activation, remaining open at rest, and closing slowly on depolarization and opening slowly in response to repolarization. Fast inactivation results in blocking the inner pore mouth with the hinged lid, where shortly after depolarization the lid closes on the mouth of the pore, blocking ion permeation. The "lid" in the hinged lid model consists of three residues within the Domain III-IV linker, isoleucine, phenylalanine, and

methionine (IFM). These hydrophobic residues are attracted to the hydrophobic residues in the pore exposed with the S4 movement. Fast inactivation may be removed by mutating the IFM motif and can be restored by adding free peptides containing the IFM motif [24,30]. Cleavage of the linker between domains III and IV has also been shown to greatly reduce fast inactivation [29,32].

2.1.6. Slow inactivation

Slow inactivation is an inactivated state distinct from fast inactivation. In the fast inactivated state the pore is "plugged" by the inactivation gate. In slow inactivation, the pore itself collapses.[33] This pore collapse has a much longer recovery period than the fast inactivated state. Slow inactivation can be distinguished from fast inactivation on the basis of kinetics and pharmacology. Fast inactivation occurs over a period of milliseconds whereas slow inactivation occurs and recovers over a period of seconds to minutes. [33] During a prolonged depolarization, the S4 segments continue to move outwards, causing the pore to collapse.

2.1.7. β subunits

The α subunit can be expressed alone to produce a functional channel; however, β subunits are important in membrane expression and gating kinetics. [34] Expression of β subunits increases rates of activation and inactivation. [34] β subunits have also been found to greatly increase membrane expression of the channel. [34]

β subunits are made up of an extracellular N terminus which contains an immunoglobulin domain and an intracellular C-terminus. [34] The immunoglobulin domain of the β subunits is structurally similar to cell adhesion molecules (CAM's). [34] β subunits can also function as CAMs and have been shown to play roles in cell migration, cell aggregation, and interact with the cytoskeleton. [34]

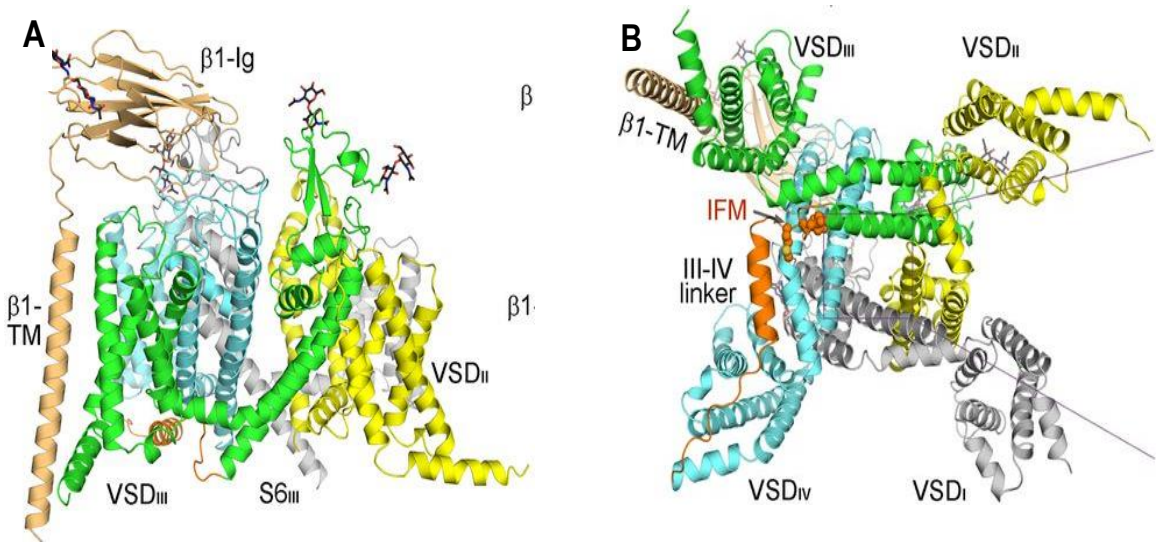

Figure 2. Structure of Nav1.4 with β1.
Figure obtained from from www.wwpdb.org. DOI: 10.2210/pdb6AGF/pdb. Adapted from original publication [35] with permission. The structure is colour coded by domain and the voltage-sensing domains are denoted VSD for each domain. The inactivation gate is shown in orange with the IFM motif depicted as a series of ball like structures. The fast inactivation gate is also labelled as the III-IV linker. The S6 domain of D3 is labelled $S6_{III}$ and the β1 complex is labelled as β1.

2.2. Non-canonical functions of voltage-gated sodium channels

VGSC are also found to a limited extent in non excitable cells like microglial cells such as astrocytes[36], oligodendrocytes[37] and Schwann cells[38], and in immune cells such as macrophages[21] and dendritic cells[39]. VGSC are also found in T lymphocytes, osteoblasts, endothelial cells and fibroblasts.[40] Their functional role in these cells is not clearly established; however, they are thought to affect endosomal acidification in phagocytic cells and podosome formation in migratory immune cells.[40]

Most of the functional data on VGSC activity in non excitable cells are from experiments using VGSC inhibitor tetrodotoxin (TTX). TTX administration blocks the pore of VGSC and prevents sodium ions from entering the channel, thus the resulting changes in cell function in the presence of TTX can be used to discuss likely VGSC functions. In astrocytes TTX increases Na+/K+ATPase activity and increases rates of apoptosis..[41] In dendritic cells, TTX administration prevents cell migration.[39] TTX can also reduce insulin release from pancreatic β cells.[42,43] In macrophages, TTX reduces

endosomal acidification and negatively impacts phagocytosis.[21] TTX also disrupts podosome formation and cell migration in macrophages. [44] In addition to disrupting function in both macrophages and microglia, TTX also increases local inflammation in surrounding tissue.[22] TTX also reduces phagocytic ability by over 40% in microglial cells.[22] These findings suggest that VGSC chiefly assist in endosomal acidification required for phagocytosis and podosome formation for cell invasion in immune cells. A role of VGSC in cell invasion is particularly interesting, as metastatic cancer cells are highly invasive[45] and have the ability to migrate rapidly through tissue microenvironments. [45]

2.2.1. Voltage-gated sodium channels promote invasiveness in immune cells

Podosomes are VGSC dependent structures that enable migratory immune cells to invade through tissue by forming actin rich protrusions in the leading edge of the cell and breaking down ECM components by secretion of matrix metalloproteases (MMPs).[46] These features enable cells capable of podosome formation to invade through tissue microenvironments.[46] Cells that contain podosomes include microglial cells[19,22] in the central nervous system and macrophages[21,22] in the rest of the body. These cells contribute to the immune response by moving rapidly through tissue microenvironments to phagocytose debris and pathogens and help to rid the body of damaged cells and infectious agents. Podosomes are simple structures characterized by an actin bundle surrounded by a ring complex. The actin core is made up of actin and several actin coordinators such as Arp 2/3, WASP, and cortactin. The surrounding ring is made up of adhesion and scaffolding proteins, and is rich in integrins, viniculin and talin.[19,47] Matrix proteins degraded by secreted MMPs include fibronectin, collagen, and laminin.[48] MMPs involved in ECM degradation include serine proteases, ADAMs (a disintegrin and metalloproteinase) or matrix metalloproteinases.[49,50] Cells with podosomes have little difficulty navigating through the basal lamina and through very dense ECM with an abundance of collagen. These features enable cells containing podosomes to digest the ECM and invade rapidly through tissue.

The function of VGSC in podosomes is the most relevant to their proposed function is in cancer cells. Podosomes are VGSC dependent structures.[44,20,21] VGSC are

abundant in podosomal membranes, where they are believed to have a functional role affecting cell invasiveness,.[21,22,44].

2.3. Voltage-gated sodium channels in cancer

De novo expression of VGSC promotes cell proliferation and invasiveness in various types of cancers. Different VGSC channel isoforms are overexpressed in different forms of cancer. According to current literature; Nav1.5 is the predominant isoform expressed in breast, ovarian, and colon cancers, Nav1.6 in cervical and prostate cancers and Nav1.7 in lung cancers.[17] All four β subunits are also detected in cancer, β1 being expressed in the greatest quantity.[17]

Expression of VGSC is linked to increased cell motility, rate of proliferation, and metastatic potential in cancer cells compared to cancer cells which do not express VGSC. In breast, prostate, and lung cancer, inhibition studies using TTX show reduced cell extension, galvanotaxis, endocytosis, migration, and cell invasion.[13–15,51] Recent studies also demonstrate that VGSC channels regulate angiogenesis of epithelial tissues near metastatic tumors.[52] The α subunit expression correlates to the metastatic potential of several cancers.[14,53] The amount of VGSC expression can be used successfully as a marker to grade tumor severity and metastatic potential. [54] Further, among patients with the same grade of breast cancer, those with elevated expression of Nav1.5 were more likely to have a recurrence or die within five years and were more likely to develop metastasis.[55] In several studies tumor grade and cancer invasiveness correlated positively with VGSC expression.[46,49] Correlation, however, does not indicate causation. It remains unclear whether VGSC expression causes cancers to become more likely to metastasize or whether VGSC expression is simply coincidental.

Experiments in which VGSC channel blockers and openers were applied to cancer cells have demonstrated that VGSC functions to increase invasiveness in cancer cells. Cell motility and cell invasiveness is reduced in the presence of TTX.[15,16,40,55,56] TTX also reduces extracellular acidification in migrating cells.[51] Impacts of VGSC on cancer cell movement have been demonstrated primarily through the use of invasion chambers to measure invasiveness and scratch assays to measure cell motility. In

breast cancer TTX reduces invasiveness in MDA-MB-468 cells and in MCF-7 cells.[57] In prostate cancer, TTX reduces invasiveness in PC3 cells. [58]

One study examined the role of VGSC inhibition on metastasis in animal models with positive results. [59] In rat models TTX administration reduced lung metastasis in prostate cancer by > 40% and increased life expectancy.[59] This study was the first *in vivo* demonstration that VGSC inhibition reduces metastasis.

2.3.1. Voltage gated sodium channels in invadopodia

In non-cancerous cells VGSC promote cell invasion by a functional role in podosomes in immune cells. It is likely then, that if cancer cells possess a similar structure VGSC may increase cell invasion in a similar fashion. In fact, cancer cells can develop structures called invadopodia, an invasive structure functionally and morphologically very similar to podosomes. Invadopodia were originally named for their ability to enable cancer cells to invade rapidly through tissue, however, some experts now think invadopodia and podosomes are the same structure entirely. [47] It appears the term invadopodia is reserved for invasive structures found in cancer cells, while the term podosomes is used for structures found in other non-cancerous cells. Due to the fact that many of the molecular markers and key functional players in podosomes are also found in invadopodia,[47] it is likely that if VGSC are expressed and play a functional role in podosomes, they may have a similar function in invadopodia in cancer cells. VGSC localization in invadopodia would explain why VGSC expression has effects on invasion and metastasis.[15,54,59]

Chapter 3.

Voltage-gated sodium channel expression in prostate cancer

3.1. Introduction

The literature states that VGSC expression increases cancer cell invasiveness, cell motility and survivability. [15,18,59,60] However, little is known as to the role VGSC may have to increase invasiveness when present. To study the characteristics, localization and functional consequences of VGSC expression in cancer I have decided to focus on prostate cancer specifically.

The literature is inconsistent as to which VGSC isoform is expressed in which cell line. It is generally accepted, based on a highly cited review article, that Nav1.6 and Nav1.7 are the predominant isoform expressed in prostate cancer of all types. [18] However, there is some contradictory evidence such as papers finding Nav1.8 or Nav1.4 or Nav1.5 are the highest isoforms expressed in PC3 cells, and some finding no Nav1.6 or Nav1.7 expression at all. [18,59,61]Since there is some contradictory evidence in the literature as to what isoforms are expressed in which type of cancer, I first sought to determine whether Nav1.6 and Nav1.7 are also the highly expressed in our paradigm.

I used patch clamping in PC3 cells to glean information on the functional aspects of the VGSC expressed in prostate cancer cells and to determine which isoform is predominantly expressed based on channel kinetics. In addition, using protocols for quantifying inward sodium currents also allowed me to conclude whether these endogenously expressed VGSC resemble traditional VGSC in structure and function.

I used qPCR and western blots to validate my findings from patch clamping and explore whether VGSC isoform expression changes depending on cell line, and various cell conditions. This will provide a comprehensive view of channel expression in PC3 and LNCaP cancer cell lines. Using qPCR I determined the amount of mRNA for each VGSC isoform (Nav1.1-Nav1.9) in several cell lines and examined whether VGSC expression changed in several different prostate cancer cell lines, in presence of a

CRISPR Rb knockout (often characteristic of a more advanced disease), and in hypoxia induced cells.

I used two cell lines to determine whether expression changed between different cell lines of the same type of cancer. PC3 cells are derived from metastatic prostate cancer that has metastasized to bone, while LNCaP cells are derived from metastatic prostate cancer that has metastasized to the lymph nodes in the neck. Both are invasive, contact independent and metastatic. [62]

Western blots were conducted for PC3 cells and LNCaP cells. 22rv1 cells were also used for comparison. 22rv1 cells are androgen therapy resistant and used to study castration resistant prostate cancer *in vitro*. Robert Payer conducted western blots for several VGSC isoforms to examine protein expression.

I used qPCR to explore VGSC expression in prostate cancer cells in hypoxic conditions to test the hypothesis that expression changes in response to different cell growing conditions. I conducted this study with LNCaP cells, under normal and hypoxic conditions and in the presence of an Rb knockout, a commonly silenced tumor suppressor in many cancers.[63] Reduced Rb expression is associated with poorer prognosis,[63–65] and often needs to occur to stimulate tumorigenesis. [65] Tumors often develop under hypoxic conditions when metabolism shifts towards anaerobic production of lactic acid and exposure to blood vessels is reduced.[66,67] Most solid metastatic tumors become hypoxic and prognosis is much poorer in hypoxic tumors. [68] Studying expression in hypoxia is relevant because hypoxia is associated with poorer prognosis and increased likelihood of metastasis. [10,68] Hypoxia is relevant when discussing how cancer cells act in tumors *in vivo*. If VGSC expression increases significantly in hypoxic conditions any findings of VGSC inhibition reducing cell invasion could be even more prominent *in vivo*. These experiments together give insight on VGSC expression in prostate cancer cells.

3.2. Methods

Cell culture

I grew all cell lines (ATCC) in their respective mediums supplemented with 10% fetal bovine serum (FBS) at 37C in 5% CO2. PC3 cells uses F-K12 media, LNCaP uses Roswell Park Memorial Institute medium (RPMI) media. All media was filtered as per ATCC recommendations. All media was stored at 4C.

Patch Clamping

Whole cell patch clamp experiments were performed at 22°C using borosilicate glass pipettes pulled with a P-1000 puller (Sutter Instruments, CA, USA), dipped in dental wax, and polished to a resistance of 1.0–1.5 MΩ. Extracellular solutions contained (in mM): 140 NaCl, 4 KCl, 2 $CaCl_2$, 1 $MgCl_2$, and 10 HEPES. Intracellular solutions contained (in mM): 130 CsF, 10 NaCl, 10 HEPES, and 10 EGTA. To ensure that any voltage elicited current was from VGSC channels I added 5 TEA (a potassium channel blocker). I titrated extracellular and intracellular solutions to pH 7.4 with CsOH.

I performed all experiments using an EPC9 patch-clamp amplifier digitized using an ITC-16 interface (HEKA Elektronik, Lambrecht, Germany). For data collection and analysis I used Patchmaster/Fitmaster (HEKA Elektronik) and Igor Pro (Wavemetrics, OR, USA) running on an iMac (Apple Inc., CA, USA). I low-pass-filtered the data at 5kHz and used a P/4 leak subtraction procedure for all recordings. The holding potential between protocols was −90 mV.

Pulse Protocols and Analysis

Macroscopic currents were elicited with 20 ms depolarizations to membrane potentials between −100 mV and +60 mV. Conductance was determined by dividing peak current by the experimentally observed reversal potential subtracted from membrane potential. Normalized conductance plotted against voltage was fit by a single Boltzmann equation.

Steady-state fast inactivation was measured as the proportion of current remaining in a test pulse to 0 mV mV following 200 ms pulses to voltages between

−130 mV and +10 mV. The normalized current plotted against voltage was fit by a single Boltzmann equation.

QPCR

Quantitative PCR (QPCR) Quantitative PCR (QPCR) was performed using SYBR Green dye on an Applied Biosystems 7300 Real Time PCR system (Applied Biosystems, Foster City, CA) (S5, S6). Briefly, 1-5 µg of total RNA was reverse transcribed into cDNA using SuperScript III (Invitrogen) in the presence of random primers or random primers and oligo dT primers. All reactions were performed with SYBR Green Master Mix (Applied Biosystems) and 25 ng of both the forward and reverse primer using the manufacturer's recommended thermocycling conditions. For each experiment, threshold levels were set during the exponential phase of the QPCR reaction using Sequence Detection Software version 1.2.2. (Applied Biosystems).

The amount of each target gene was determined for each sample using the comparative threshold cycle or Δ**Ct** method. Since gene expression is being compared within the same cell line, with no treatment condition, ΔCt was calculated using the relative quantification method. [69] Data is represented as $2^{-\Delta Ct}$ following the analysis protocol described in Relative Quantification. [69] This enables comparison of mRNA expression of target genes within the same cell line.

An ANOVA test was run on JMP (SAS institute) to determine whether ΔCt values were significantly different between VGSC isoforms and which VGSC isoform was expressed in the highest quantity. Significance was determined by comparing ΔCt values between VGSC isoforms. A Post Hoc test was used to determine which isoform in question was significant.

Primers used:

SCN1A	F 5'-CAGTGCAGCAGGCAGGC	R 5' - TCAATCGGTTCCCTTCA
SCN2A	F 5' AGACTTCAGTGGTGCTGG	R 5' - CTCTTCTTCTCCAGACTG
SCN3A	F 5' GGGTTAGGAGAGCTGTTGG	R 5' CAAGGTGCTCTCTCTGTCTTC

SCN4A	F 5’ CTCGAGCTGGACCACCTT	R 5’ TCTCCTCTGCCTGCTCCTC
SCN5A	F 5’ CAACAGCTGGAATATCTTCG	R 5’ CCAAAGATGGAGTAGATGAAC
SCN8A	F 5’ TCAGCATCCCAGGCTCGC	R 5’ CTGGCTGTAGCCGCTGTA
SCN9A	F 5’ - TCAGGTTTCCCATGAACAGC	R 5’ - TCAGGTTTCCCATAACAGC
SCN10A	F 5’ - GTTGGCACAGCAATAGATCTCC	R 5’ - GACAGCCATGTCATTCTTGAC
SCN11A	F 5’ - CCATCCTTGACCATCTCAACTG	R 5’ - GGAAAGGAATGTGCTCCTGA

Western blots

Whole cell extracts were lysed and transferred to a polyvinylidene difluoride membrane using a transfer apparatus according to the manufacturer’s protocols (Bio-Rad). After incubation with 5% nonfat milk in tris buffered saline (TBS) (10 mM Tris, pH 8.0, 150 mM NaCl, 0.5% Tween 20) for 60 min, the membrane was washed three times with TBS (10 min per wash) and incubated with antibodies against Nav1.1, Nav1.4, Nav1.5, Nav1.6, and Nav1.7 (1:2000), beta tubulin (1:2000), at 4 °C for 15 h. Membranes were washed three times with TBS (10 min per wash) and incubated with a 1:3000 dilution of horseradish peroxidase-conjugated anti-mouse or anti-rabbit antibodies for 2 h. Blots were washed with TBS three times and developed with the SnapGene (https://www.snapgene.com/)according to the manufacturer’s protocols.

3.3. Results

3.3.1. Endogenous sodium current recordings in PC3 cells

I used patch clamp experiments to determine whether the endogenously expressed channels conform to the expected biophysical properties of VGSC and whether the endogenous channels have the properties of a neural channel VGSC isoform.

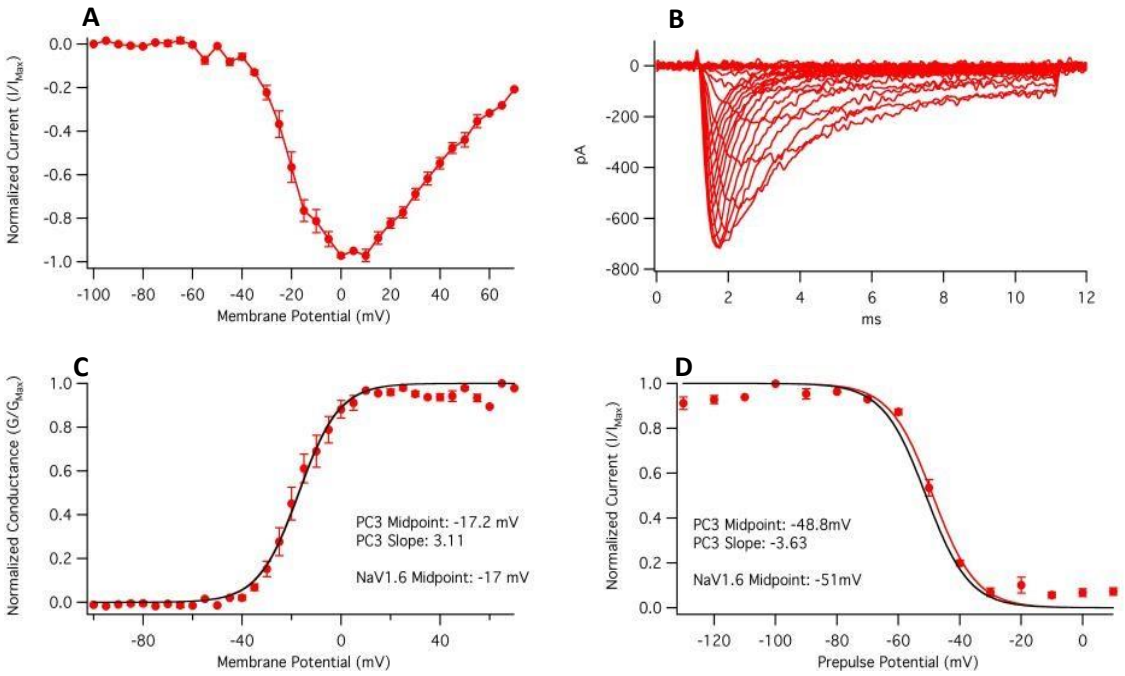

Figure 3. VGSC expressed in prostate cancer cells are abundant an exhibit typical voltage-gated sodium channel properties.

Patch clamp data from PC3 cells. A. An IV curve (N=5) showing peak current at different membrane potentials. B. A current trace from PC3 cells showing channel opening and inactivation typical of voltage gated sodium channels C. A GV curve showing number of channels open at various membrane potentials. Normalized conductance is plotted against membrane potential. D. A FI curve showing channel inactivation at various membrane potentials. Midpoint and slope values of GV and FI curves were found to be most similar to Nav1.6, a neuronal sodium channel.

My data shows that these endogenously expressed channels have the biophysical properties of voltage gated sodium channels. The endogenously expressed channels have propeties typical of VGSC expressed in human neurons. Published midpoint and slope values for different VGSC isoforms were compared to experimental data using the Boltzmann equation. Nav1.6 appears to be the predominantly expressed isoform in PC3 cells based on patch clamp experiments. The midpoint of Nav1.6 in the GV curve (**C**) is -17 mV and in our experimental data from PC3 cells the midpoint we got was -17.2 mV. From the fast inactivation curve (**D**) the accepted midpoint value for an FI curve of Nav1.6 is -51 mV and the experimental value I obtained is -49 mV. Nav1.6 is therefore the most likely channel isoform expressed in prostate cancer cells based on the biophysical data.

3.3.2. mRNA expression profiles for voltage-gated sodium channel isoforms in PC3 and LNCaP cells

I performed qPCR experiments to examine whether isoform expression changed depending on cancer cell type. Patch data suggested that PC3 cells express Nav1.6 (of the SCN8A gene) exclusively. I conducted qPCR in PC3 cells and LNCaP cells to determine whether the same isoforms were expressed in different prostate cancer cell lines.

Expression of isoforms is compared within each cell line. No control was used as these channels are expressed endogenously in cancer cells. I strove to examine whether VGSC were present, and which isoforms were abundant.

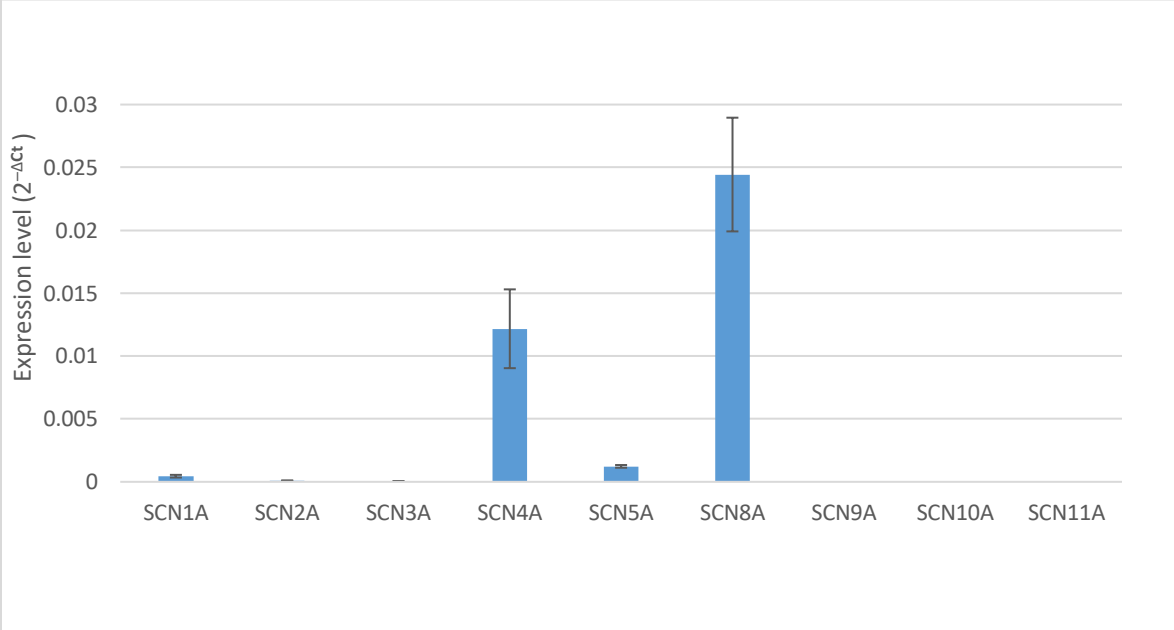

Figure 4. mRNA expression of VGSC isoforms in PC3 cells.
SCN8A is expressed significantly higher than other VGSC isoforms at $p<0.0001$. ($P<0.05$). SCN4A is also expressed in PC3 cells, but in smaller amounts. SCN1A-3A, SCN9A -10A were not expressed. VGSC isoform expression is represented as $2^{-\Delta Ct}$ values to compare expression within the same cell line.

Results from qPCR experiments confirm that SCN8A (Nav1.6) is the predominant isoform expressed in PC3 cells. Of note is the expression of SCN4A. SCN8A is more significantly expressed over any other isoform at p<0.0001. (P<0.05).

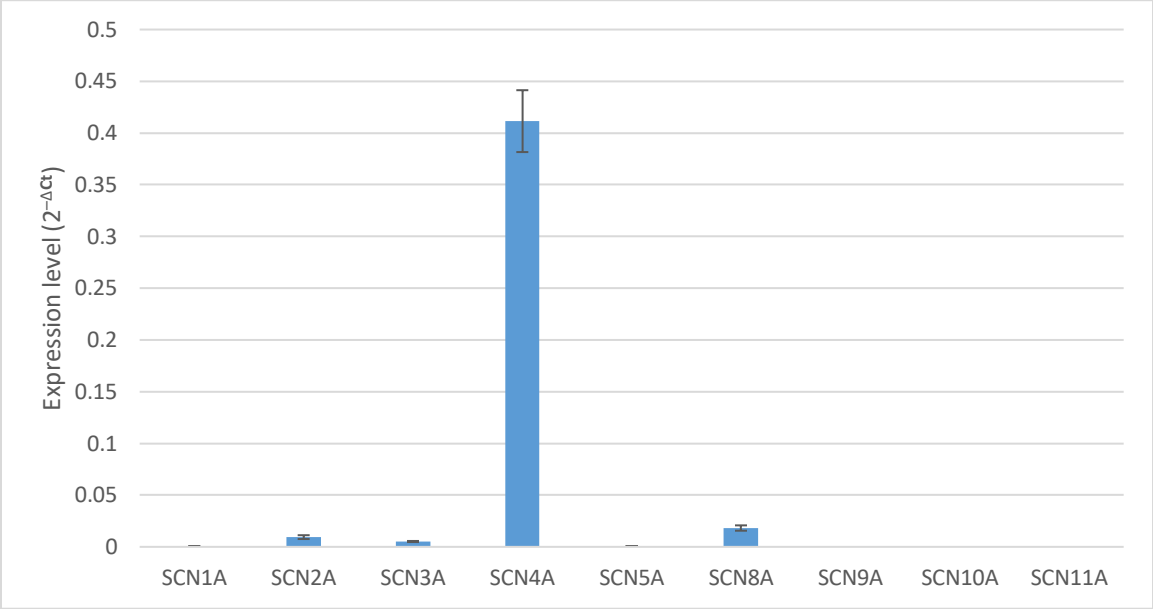

Figure 5. mRNA expression of VGSC isoforms in LNCaP cells.
SCN4A (Nav1.4) is the highest expressed VGSC channel with only trace amounts of other isoforms. SCN4A expression is significantly higher than any other isoform at p<0.0001. (p<0.05) Data is represented as $2^{-\Delta Ct}$ values to compare the expression of different isoforms in the same cell line. .

In LNCaP cells the highest expressed isoform is Nav1.4 or SCN4A, overexpressed significantly at p<0.0001. Trace amounts were found of SCN1A-3A, SCN5A-8A. SCN9A-11A were not expressed.

3.3.3. Protein expression profiles for voltage-gated sodium channel isoforms in PC3 and LNCaP cells

In addition to qPCR, Western blots were conducted by Robert Payer from Dr. Tim Beischlag's lab. Western blots were used to measure the relative amount of protein expression, whereas qPCR is used to quantify mRNA expression. I was interested in whether findings from Western blots matched my findings from qPCR. Western Blots were conducted for PC3, LNCaP and 22RV1 cells. Included are western blots of Nav1.6 and Nav1.4. (Figure 4 and Figure 5).

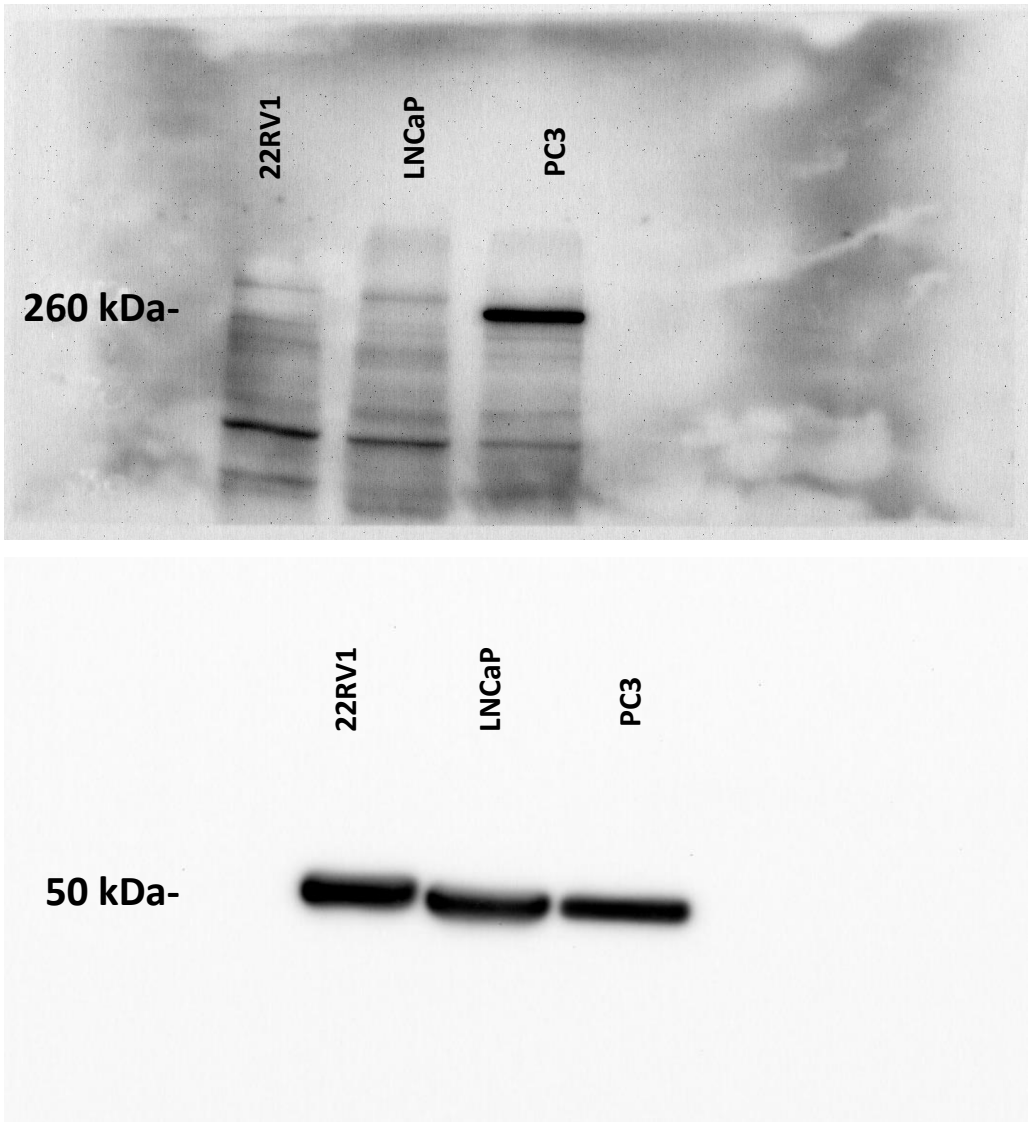

Figure 6. Nav1.6 is expressed in PC3 cells.
Western blot of Nav1.6 in 22RV1, LNCaP and PC3 cells. Right to left; LNCaP, 22RV1 and PC3 samples. Top: Nav1.6, bottom beta tubulin which was used as a control. Nav1.6 is highly expressed in PC3 cells but not found in LNCaP or 22RV1 cells. Band at 260 kDa clearly visible in PC3 cells.

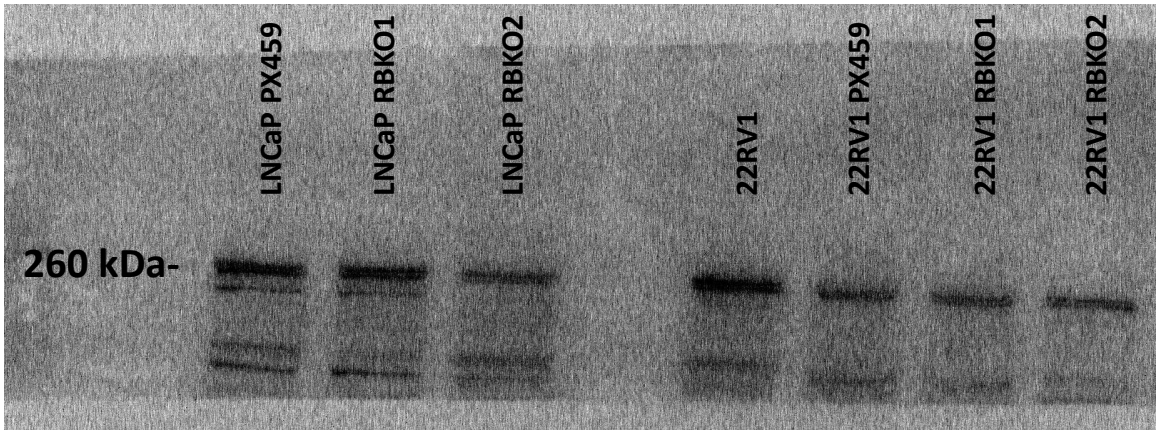

Figure 7. Nav1.4 is expressed in LNCaP and 22RV1 cells.
Western blot of Nav1.4 in (left three columns) LNCaP cells and (right four columns) 22RV1 cells. Cell samples (left to right) LNCaP cells; PX459 vehicular control, Rb knockout 3B1, Rb knockout 4C3, 22RV1 cells; PX459 vehicular control, Rb knockout 2B5, Rb knockout 3C4, Rb knockout 4A2.. Presence of band at 260 kDa clearly visible in all LNCaP and 22RV1 cell lines. No change in Nav1.4 protein expression in the presence of Rb knockout.

Interestingly Nav1.6 expression differed between PC3 and LNCaP cells. Nav1.6 was expected to be the highest expressed isoform in all prostate cancer cell lines. Rather, expression is different between different cell lines. Western blots showed expression of Nav1.4 in LNCaP cells, and showed Nav1.6 expression in PC3 cells.

3.3.4. Effects of hypoxia and tumor suppressor knockouts on voltage-gated sodium channel expression

I examined changes to VGSC expression in hypoxia and in presence of an Rb knockout using qPCR. All isoforms were tested (SCN1A-SCN11A) in control and two Rb knockout cell lines. Only SCN4A data was deemed relevant due to the extremely low expression of other channel isoforms. (Figure 8) Experiment was conducted as a triplicate.

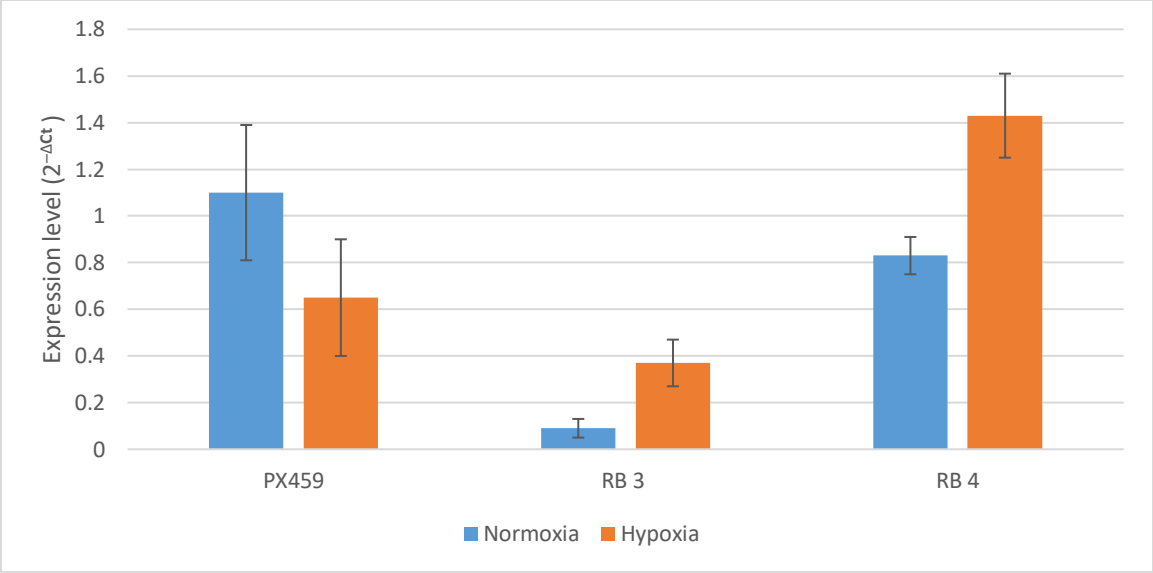

Figure 8. mRNA changes to SCN4A expression in hypoxia and in the presence of a Rb knockout.

PX459 cells are vehicular control cells and RB 3 and RB 4 are two separate Rb KO cell lines. All cell lines are generated in LNCaP cells. In Rb knockout lines (RB3 and RB4) expression is significantly higher with hypoxia at $p=0.0492$ ($p<0.05$).

In PX459 cells there was no significant change to SCN4A expression between hypoxia and normoxia conditions at $p=0.1121$. Effect of hypoxia was not significant ($p>0.05$). However, when cell line was controlled for as a random effect, (i.e. the difference in effects between RB3 and RB4 cell lines) hypoxia had an effect. In Rb knockout lines (RB3 and RB4) expression is significantly higher with hypoxia at $p=0.0492$.

It is unclear whether there is any prominent effect on VGSC expression with the addition of an Rb knockout or with exposure to hypoxia.

3.3.5. Voltage-gated sodium channel expression in metastatic, castration resistant and neuroendocrine prostate tumors

Our colleague Dr. Nader Al Nakouzi at the Vancouver Prostate Centre conducted an immunohistochemistry experiment to explore VGSC expression in prostate tissue slices. Nav1.6 antibody was used, after our preliminary data suggested it likely to be a predominant isoform. Nav1.6 expression patterns are presented in terms of immunohistochemical intensity. (Figure 9).

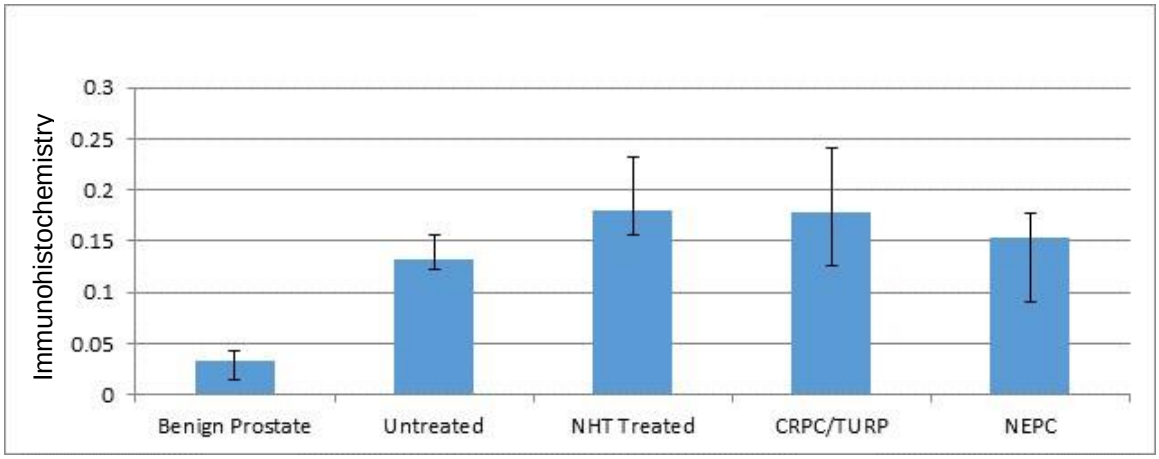

Figure 9. VGSC expression increases in metastatic prostate cancer.
Comparison between Nav1.6 expression in benign prostate, untreated prostate cancer, and increasingly aggressive types of prostate cancer. (NHT = hormotherapy; CRPC= castration resistant; NEPC= Neuroendocrine). Experiment conducted in rat prostate tissue slices taken from several rats from each condition. Expression is shown in immunohistochemistry intensity and compared between different grades of tumor severity. Expression is elevated even in castration resistant and neuroendocrine prostate cancer.

Data from rat tissue slices shows that VGSC channel expression is increased in malignant prostate cancer tumors compared to benign prostate tumors. Additionally, this elevated expression remains throughout all stages examined, and does not decrease even in later stages such as hormone treated, castration resistant, or neuroendocrine prostate cancer..

3.4. Discussion

My results suggest that metastatic prostate cancer cells express VGSC channels, and isoforms expressed can differ depending on cell type and growing conditions. Comparison between prostate cancer cells derived from bone metastasis (PC3 cells) and lymph metastasis (LNCaP cells) shows that VGSC channels expression is present and upregulated, though the exact isoform expressed are different (Nav1.6 in PC3 and Nav1.4 in LNCaP cells). It is interesting that different VGSC isoforms are expressed in different prostate cancer cell lines.

.

Immunohistochemistry data demonstrates that VGSC expression increases in metastatic prostate tumors relative to benign prostate tumors. Further, and perhaps most importantly, this increased expression of VGSC is maintained throughout even the latest stages of the disease.

It is noteworthy that the isoform examined was Nav1.6, which, after our findings from qPCR that different isoforms may be expressed in different cell lines, may not be the only isoform expressed in metastatic disease. Results may have been more significant if a pan-VGSC antibody that is not isoform specific was used. This may be relevant to discussion of VGSC as a potential therapeutic as expression does not disappear even in the latest stages of the disease.

Data from patch-clamping suggest that the sodium channels expressed in prostate cancer cells closely resemble human neuronal voltage gated sodium channels. They are activated in response to a depolarization of membrane potential and current traces exhibit exponential decay, characteristic of VGSC channel inactivation. In PC3 cells the activation and inactivation curves are closest to the Nav1.6 isoform, which is confirmed by data from qPCR to be the predominant isoform in our paradigm. Western blots confirm that VGSC expression differs between cell lines in that PC3 cells preferentially express Nav1.6 and LNCaP cells and 22RV1 cells preferentially express Nav1.4.

Cell differences may select for a particular VGSC isoform over another, such as Nav1.4 over Nav1.6 in LNCaP cells. Both LNCaP and PC3 cells are prostate derived, however they bear different characteristics and grow in different types of medium. In addition, it is interesting that there has been such conflicting data on a simple qPCR assay to determine which VGSC isoforms are expressed depending on what laboratory conducts the experiment.

The literature is inconsistent as to which VGSC isoform is expressed in which cell line. Some studies have reported that Nav1.8[61] is expressed the highest in PC3 cells, while some studies have said that Nav1.7[70] or Nav1.6[14] is the highest expressed, and some argue that Nav1.1[61], Nav1.2[61], Nav1.5[61] and Nav1.6[14,61] are also expressed highly. In LNCaP cells some studies have reported that Nav1.8[61] is the highest isoform expressed, with Nav1.5[61], Nav1.6[61], and Nav1.7[61] also expressed highly, and some

argue that Nav1.4[58] is the only isoform expressed and no other isoforms were found in any measurable quantity.

My results demonstrate that, depending on cell type and growing conditions, the predominant isoform can differ. In my experimental paradigm, PC3 cells expressed predominantly Nav1.6 withsome Nav1.4 expression and LNCaP cells expressed Nav1.4 almost exclusively. This may not be an inconsistency due to poor data collection, but rather, may be due to the ability of prostate cancer to select for particular isoforms depending on cell growing conditions. Even in the same cell line, different laboratory conditions may select for different isoforms. This would explain why different laboratories have reported such different findings for VGSC expression.

Laniado et al. conducted the first patch-clamp experiments in PC3 and LNCaP cells, in one of the most highly cited research publications when discussing the characteristics of VGSC in prostate cancer. [71] Laniado et al. determined that in PC3 cells only 10% of cells express functional VGSC. [71] They also reported that LNCaP cells display no VGSC expression whatsoever and displayed no inward sodium currents from patch-clamp recordings. [71] This low percentage of cells expressing VGSC was demonstrated using flow cytometry cell sorting. [71] It was suggested that VGSC expression may be regulated by phosphorylation or dephosphorylation, or an abnormal mutation or glycosylation that inactivates the channels under certain conditions. [71] The patch-clamp data reported from the 10% of PC3 cells expressing VGSC shows a large inward sodium current followed by characteristic VGSC inactivation and has been the cited research in many review papers discussing VGSC expression in prostate cancer.

Our data agrees with certain findings from Laniado et al. and also disagrees with certain findings. My reported patch-clamp data for PC3 cells displays similar current traces and channel kinetics to the data collected by Laniado et al. The overall shape and size of the reported current traces were comparable to my findings. The midpoint and slope values of the conductance (GV) curve were not explicitly reported, but the midpoint on the graph appears to be approximately -20 mV. [71] -20 mV is similar, but slightly left shifted compared to my reported finding of -17.2 mV, The fast inactivation curve (FI) was not reported and thus cannot be compared. Laniado et al. reported no LNCaP VGSC expression whatsoever, which our data disagrees with. While I did not conduct electrophysiological recordings of LNCaP cells, I conducted several qPCR and western

blot experiments that all showed expression of Nav1.4 in LNCaP cells. Based on my data LNCaP cells do express VGSC. In addition, their western blot differs from my results. Their western blot shows no clear band at 260kDA, the band is very faint, which they explained by saying that only 10% of cells contain the protein. In my data however, I found that there was a prominent band in PC3 cells and a more faint (but still very visible) band in LNCaP cells.

Laniado et al. suggests that the reason why only 10% of cells have significant VGSC expression is due to a mutation or glycosylation that selectively changes membrane expression of VGSC throughout the cell cycle. [71] While I am skeptical that a mutation or glycosylation would be capable of achieving this, it remains possible that phosphorylation or secondary messenger signalling may in some way, alter channel activity depending on the conditions in the cell. This would fit with my theory that VGSC are expressed in invadopodia, structures that are transient, and only found in the leading edge of an invading cell. If my theory is correct, VGSC would not be found in fully adhered, non migratory cells. In the patch data I collected it is clear that PC3 cells express endogenous VGSC. However, while some cells showed an abundant amount on inward sodium current, many of the cells I examined contained a smaller amount of current, with some cells showing no current at all. This fits with my theory of expression in a transient structure that is prominent in motile cells, and may be absent or hardly apparent in fully adhered, stationary cells.

Fraser et al. conducted patch clamp recordings in breast cancer MDA-MB-231 cells and showed that VGSC current was apparent, TTX sensitive, and similar to the current traces found by Laniado et al.[15] Fraser et al. also conducted patch-clamp recordings on three other cell lines, MCF-10A, MCF-7 and MDA-MB-468 cells in addition to MDA-MB-231 cells, none of which displayed significant inward current. [15] While this study was conducted in breast cancer cells, and thus less applicable in discussing prostate cancer, findings from this paper may still be relevant. It is interesting that researchers are finding certain cell lines expressing an abundance of VGSC, and some cell lines expressing none at all.

My data disagrees with the finding that LNCaP cells contain no functional VGSC and agrees with the finding that PC3 cells exhibit traditional VGSC properties. My data supports the literature that found Nav1.6 expression in PC3 cells and Nav1.4 expression

in LNCaP cells with the caveat that certain laboratory growing conditions such as cell line and media used for culture may alter isoform expression.

Limitations of this study include the lack of control samples for both qPCR and western blot experiments. Because VGSC are endogenously expressed in metastatic cancer lines, I compared isoform expression within different metastatic cell lines and had no control sample. This experiment could be repeated using non-malignant prostate epithelial cells, benign prostate tumor cells or another cell line that would serve as a control for comparison purposes.

In summary, VGSC are endogenously expressed in PC3 and LNCaP cells and exhibit channel gating kinetics typical of a VGSC. Isoform expression may differ in different cell types. This observation suggests that it is not the presence of a particular VGSC isoform, but the presence of VGSC in general that may impart function and survivability to prostate cancer cells.

Chapter 4.

Voltage-gated sodium channels localize in invadopodia in prostate cancer cells

4.1. Introduction

Voltage-gated sodium channels (VGSC) may play a role in the function of invadopodia[19,44,72], invasive structures in the leading edge of migrating cancer cells. Invadopodia are actin rich protrusions of the cell that degrade the extracellular matrix (ECM) through release of enzymes and proteases which allow cells to invade and move through tissue. [19,47] A functional role of VGSC in invadopodia would explain why inhibiting VGSC has an impact on invasiveness and metastasis in cancer. [15,16,40,55,56]

I hypothesized that VGSC are localized in invadopodia and have conducted immunocytochemistry experiments to test this idea. My previous data shows that the predominant VGSC in PC3 cells is Nav1.6, and thus I have used a Nav1.6 specific antibody to image PC3 cells and determine VGSC localization. First, I examined VGSC localization in relation to the F-actin cytoskeleton. Second, I examine colocalization with invadopodia by conducting a co-localization analysis with vimentin, a protein that is found exclusively in the leading edge of the cell.

Vimentin is required for invadopodia to anchor to the actin cytoskeleton and intermediate filaments in the cell. [73,74] Disrupting vimentin anchoring to plectin, intermediate, filaments, and F-actin severely impacts formation of invadopodia as well as measured functions of invadopodia activity such as extracellular matrix (ECM) degradation, cell migration and metastasis. [73] Vimentin localization in the cell determines the organization of invadopodia and lamelliopodia (ruffled membranes in the leading edge) during cell migration and cell invasion. [75] In addition to a functional link to invadopodia, vimentin is exclusively found in the leading edge of a migrating cell. [76] These features make vimentin ideal for visualizing invadopodia localization in the cell.

To invade through tissue microenvironments a cell must first develop invadopodia, small actin rich protrusions that secrete matrix metalloproteases (MMPs) and digest components of the eECM and the basement membrane. Invadopodia will

form small protrusions that elongate, mature and extend into the basement membrane or surrounding tissue, enabling the cell to invade. It is in this elongation and maturation step that vimentin is required. [75] After invadopodia maturation, metastatic cancer cells can migrate away from the primary tumor site and into surrounding tissue.

There have been three papers that have suggested VGSC play a role in invadopodia. A review paper by Besson et al. has come to the same conclusion that I have that a role in transient invasive structures would be a neat explanation for the effects of VGSC and cell invasion in cancer.[77] The papers cited as evidence for that conclusion include two papers where VGSC were found to be situated near the sodium hydrogen exchanger (NHE) in cancer cells. [72,78] NHE are found in every cell in the body and have a variety of functions in the cell. [79] NHE may be involved in invadopodia, or it may not. By using vimentin, a protein that is not found in the cytosol and is not likely to have alternate functions beyond invadopodia maturation, I wanted to reduce the chance of making false conclusions as much as possible.

This study is the first to use vimentin to explore VGSC localization in cancer of all types and the first to show VGSC localization in invadopodia in prostate cancer.

4.2. Methods

Cell culture

I grew all cell lines (ATCC) in their respective mediums supplemented with 10% fetal bovine serum (FBS) at 37° C in 5% CO2. PC3 cells uses F-K12 media, LNCaP uses Roswell Park Memorial Institute medium (RPMI) media, DU145 uses Dulbecco's Modified Eagle's Medium (DMEM), All media was filtered as per ATCC recommendations. All media was stored at 4° C.

Immunolabelling

Cells were fixed in 4% paraformaldehyde for 10 min and permeabilized with 0.1% Triton X-100 for 10 min. After blocking with 10% NGS for 1 hour, cells were incubated with anti-Nav1.6 (mouse monoclonal IgG, Thermo Fisher), and anti-vimentin (rabbit monoclonal IgG, Thermo Fisher) antibodies overnight at 4C. After washing, incubation with Alexa 488 secondary antibody (anti-mouse IgG, Thermo Fisher) and Alexa 647

secondary antibody (anti-rabbit IgG, Thermo Fisher) The antibodies were used in 1% BSA-PBS solution. Actin labeling was performed by Phalloidin conjugated to Alexa 647 (Sigma). Coverslips were mounted with Prolong Gold Antifade Reagent (Thermo Fisher). Cells were then examined using a Nikon Ti-E inverted microscope equipped with an Andor Zyla5.5 camera 159 and NIS image acquisition software. The image of actin and Nav1.6 was collected on a Nikon A1R laser scanning confocal microscope and a 60X 1.4 NA Oil lens for further clarity.

Immunocytochemistry

Immunocytochemistry experiments were performed using 80 % confluent 60 mm dishes of PC3 cells. PC3 cells were grown in DMEM Medium supplemented with 10 % FBS on 13 mm round glass coverslips. Cells were fixed with 4 % paraformaldehyde in phosphate buffered saline (PBS) for 10 minutes at room temperature and washed 1x in PBS for 10 min. Cells were then permeabilized with Triton X for 10 minutes, washed 1x in PBS, and then incubated with 10 % normal goat serum in PBS for 1 h at room temperature. Cells were incubated overnight with primary antibodies directed against the DI-DII linker of $Na_V1.1$ (ASC-001 Alomone labs; 1:300 dilution in PBS supplemented with 10% normal goat serum). Cells were washed 3x with PBS and then a secondary antibody (CFL-488, goat-anti-mouse; Santa Cruz Biotechnology; 1:500 dilution in PBS) was applied for 1 h at room temperature. A Hoechst 33342 (1:500 dilution PBS) stain was applied for 10 minutes, and cells were mounted with Prolong Gold reagent (Molecular Probes, Invitrogen) onto glass slides. Images were collected using a Nikon Ti-E inverted microscope equipped with an Andor Zyla5.5 camera and NIS image acquisition software. Slides were imaged with a 40x 1.35NA objective. Analysis was performed using FIJI: An open source platform for image analysis. Mean intensity information was collected per cell, using Hoechst stain to count cells. Colocalization analysis was conducted on FIJI Coloc 2 analysis software and significance determined using JMP (SAS institute).

4.3. Results

4.3.1. Visualizing Nav1.6 expression in PC3 cells

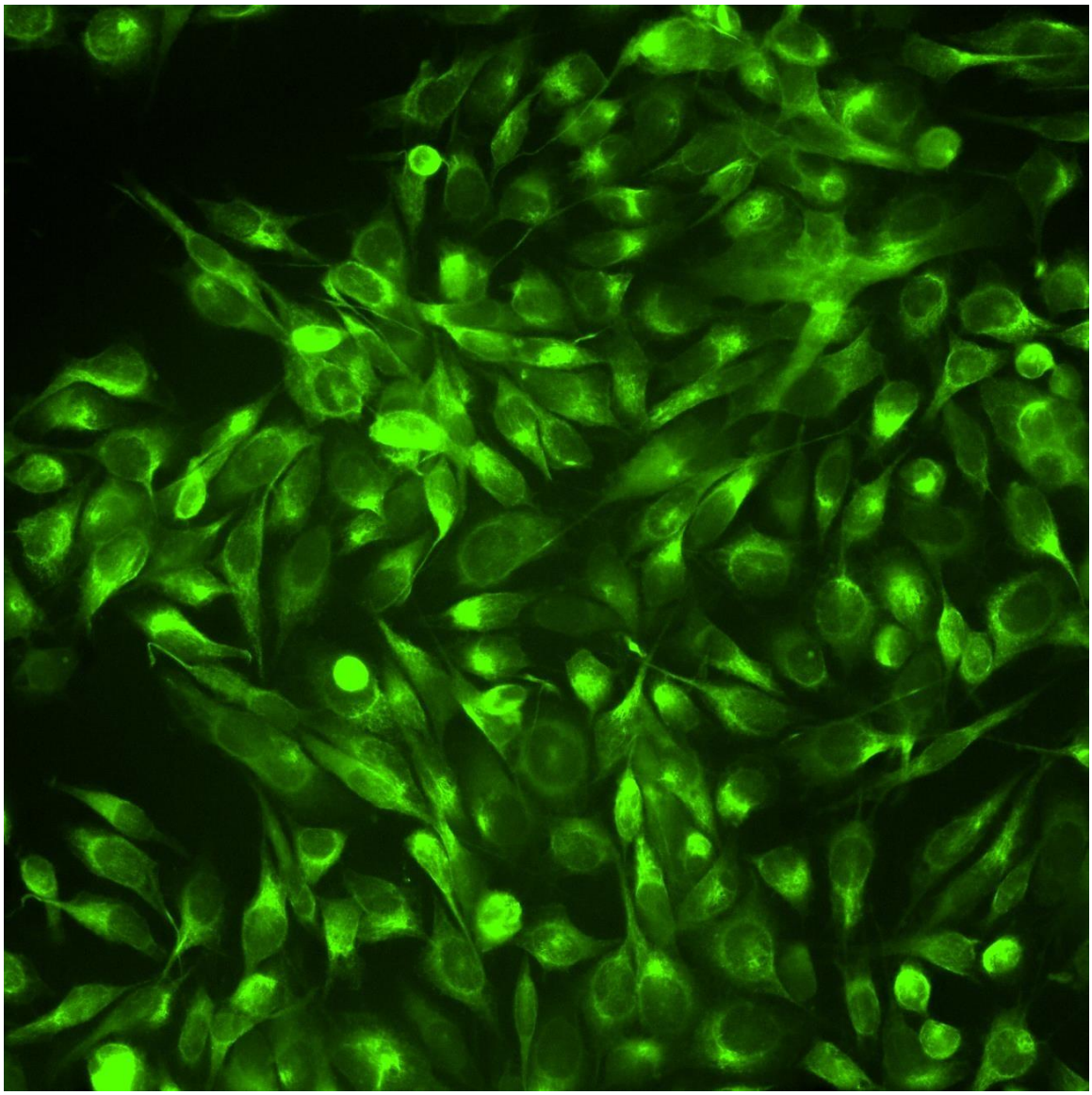

Figure 10. Nav1.6 expression in PC3 cells appears to be polarized.
Nav1.6 specific monoclonal antibody in Alexa 488 (Green) was imaged in fully adhered cells at a high confluence. Note that Nav1.6 appears to be polarized in many cells, tending to one side of the cell as opposed to distributing evenly all over the cell.

Images of Nav1.6 in PC3 cells (obtained using a fluorescent microscope) show what appears to be polarized expression of Nav1.6. From this figure I gathered that Nav1.6 expression was present in PC3 cells and that expression appeared to be

concentrated more in one area of cell. To gain a clearer picture of expression patterns I repeated Nav1.6 staining along with F-actin, a marker of the cytoskeleton to clearly visualize Nav1.6 in relation to the contours of the cell. I used a confocal microscope to obtain a higher resolution and clearer picture to be able to discuss Nav1.6 localization in the cell.

4.3.2. Nav1.6 localization in PC3 cells in relation to the actin cytoskeleton

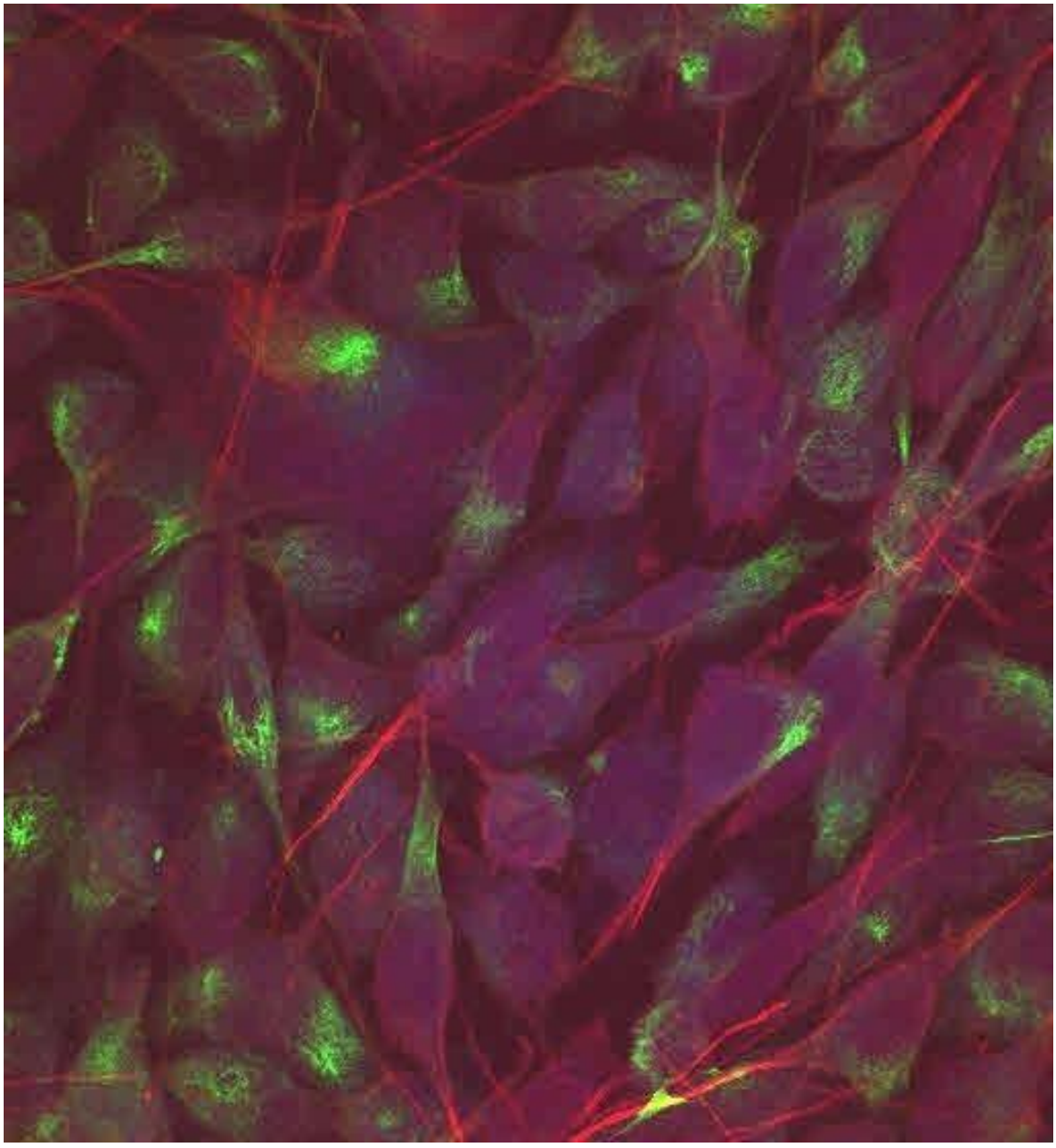

Figure 11. VGSC localization is polarized in PC3 cells.
Confocal image of PC3 cells with Nav1.6 monoclonal specific antibody in green, phalloidin (F actin) stained in red. Hoescht, the nuclear stain, is visible in blue. Nav1.6 antibody was left on for a shorter amount of time to reduce any noise and imaged using a confocal microscope for clarity.

I collected images to test the hypothesis that VGSC localize in the leading edge of the cell. Nav1.6 appears to tend towards one side of the cell, with some cells displaying a large quantity of Nav1.6 and some displaying none whatsoever (Figure 10). To obtain clearer information on VGSC localization in relation to the nucleus and contours of the cell I re-imaged Nav1.6 in PC3 cells in the presence of F-actin and using a confocal microscope to reduce noise (Figure 11).

These data demonstrate that Nav1.6 is not expressed over the entire surface of the membrane, as is often seen in transfected cells but rather, in a polarized manner. Nav1.6 preferentially expresses towards one side of the cell, which can be seen in almost every cell in Figure 11. Interestingly, some cells display no Nav1.6 at all. This could be indicative of VGSC taking part in transient structures during cell migration and becoming absent in fully adhered, non migratory cells.

4.3.3. Nav1.6 localization in the leading edge of PC3 cells

To test the hypothesis that Nav1.6 is found in invadopodia, I conducted further experiments using a marker of invadopodia maturation (Figure 12 and Figure 13). Vimentin (red) and Nav1.6 (green) were used to determine if Nav1.6 colocalizes with invadopodia. Where Nav1.6 (green) colocalizes highly with vimentin (red), the figure appears yellow.

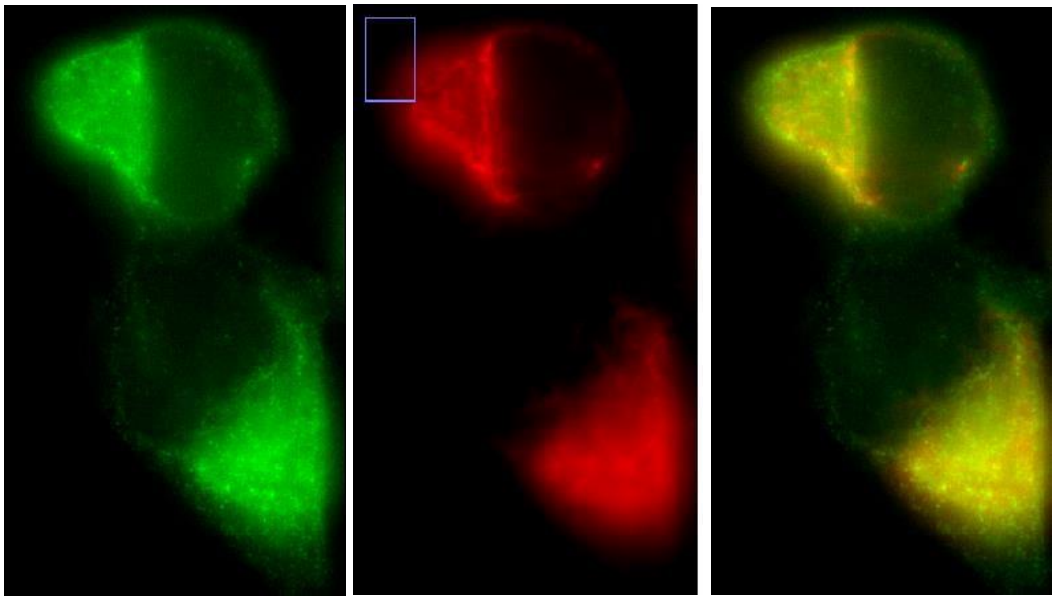

Figure 12. VGSC colocalize with vimentin.
Nav1.6 (Green) and vimentin (Red). On the right the two images are superimposed, where yellow denotes anoverlap between Nav1.6 and vimentin, a marker of the leading edge.

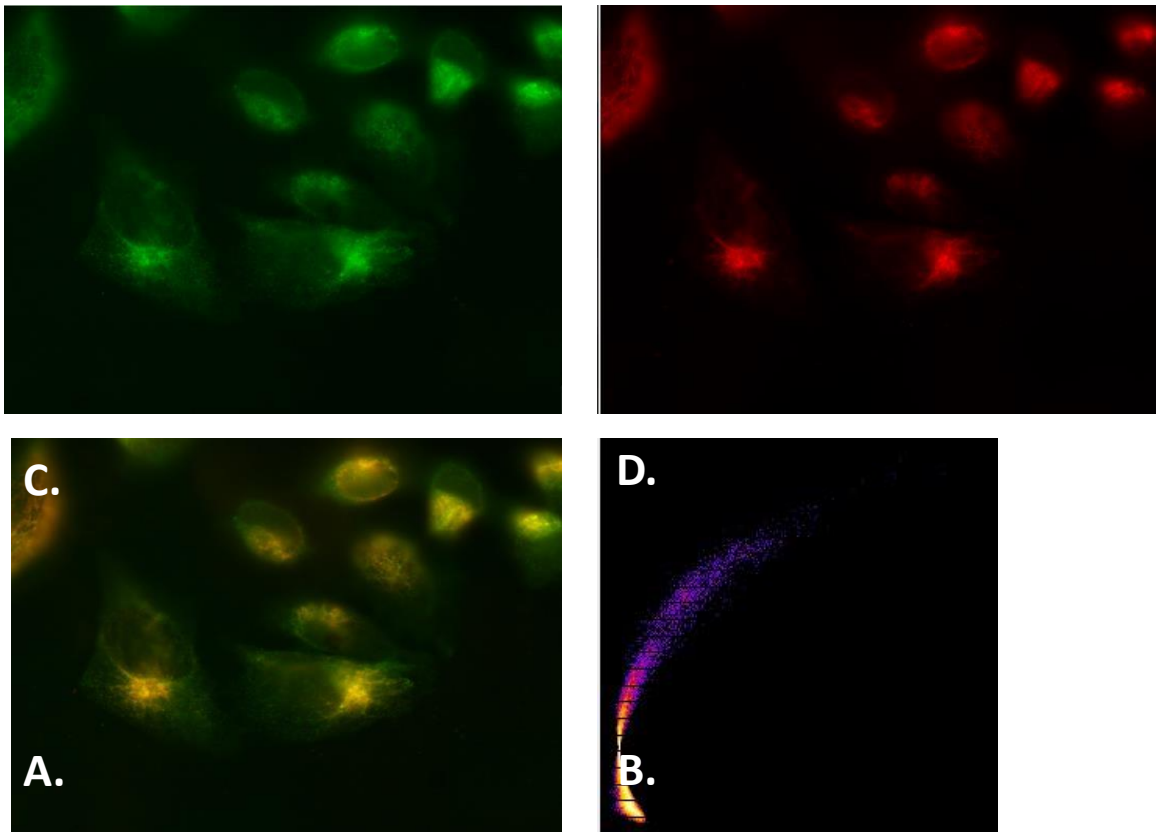

Figure 13. VGSC are found in invadopodia.
A-B. Colocalization analysis for Nav1.6 and Vimentin. Nav1.6 (green) localization is compared to vimentin (red). **C.** Bottom figure shows the two overlapped where yellow denotes anoverlap between red and green. To the bottom right is a sample of a correlation analysis scatterplot for one cell pictured bottom right. **D.** An example of a scatterplot from the colocalization analysis. (N=87)

Visually, Nav1.6 appears to colocalize highly with vimentin. This can be seen even in very large groups of cells. (Figure 13). Statistical analysis of PC3 cells (N=87) reveals that Nav1.6 and vimentin colocalize strongly. Colocalization analysis for vimentin and Nav1.6 in PC3 cells yields a Pearson correlation coefficient of .93/1. This is significant at $p < 0.0001$. ($p<0.05$). This data demonstrates that Nav1.6 is found in close proximity to invadopodia in the cell.

4.4. Discussion

This study is shows that Nav1.6 colocalizes with vimentin in PC3 cells. This suggests that VGSC may colocalize with vimentin in other prostate cancer cell lines and may suggest that VGSC are found in close proximity to invadopodia in prostate cancer cells. VGSC are not expressed uniformly over the surface of the cell as would be expected in a cardiomyocyte or transient transfection, but rather, cluster off to one side of the cell. Expression of VGSC appears to be polarized with VGSC tending to one side of the cell over another.

PC3 cells and Nav1.6 were used due to the high expression of VGSC in PC3 cells and the high amount of Nav1.6 protein, reducing the likelihood of ambiguous results, either with the possibility of a large number of alternate isoforms that may not have been stained, or having to use a antibody that is not as specific and may have alternate targets in the cell. A limitation of this study is that only PC3 cells were used to collect imaging data. Alternate cell lines in other forms of prostate cancer were not examined. Other forms of cancer were also not examined, reducing the findings of this paper to be only applicable to discussion of prostate cancer cells.

Further, I conducted this study using vimentin as a marker of invadopodia, however, the experiment could have been repeated in other markers of invadopodia to further validate findings. The discussion of the results of this experiment rely on the

implication that vimentin is found in invadopodia and the antibodies used have no off target effects.

In 2015 Besson et al. published a review article on VGSC in cancer and became the first to publish on the theory that VGSC may be found in invadopodia.[77] They used the fact that VGSC expression correlates strongly with cancer aggressiveness, with more aggressive cancers displaying a higher expression as a basis for the theory of a functional role of VGSC in cell invasion. They cited a paper that VGSC colocalize with NHE in lipid rafts in breast cancer, which are thought to contain caveolin,[78] a key player in endocytosis by formation of caveolae and signal transduction that may participate in the formation of invadopodia. A functional role of caveolin in invadopodia has been implied, but remains to be determined. [78] The lines of evidence that caveolin may be found in invadopodia, that NHE may have a functional role in ECM, and Nav1.5 is found nearby caveolin and NHE was used as evidence to conclude that VGSC is likely to exist in invadopodia.

One of the papers cited by Besson et al., and one of the first publications to discuss the idea of VGSC in a functional role in invadopodia is that of Brisson et al. who in 2013 discovered that NHE and Nav1.5 coprecipitate in breast cancer. They published co-immunoprecipitation data as well as imaging pictures of NHE and Nav1.5 being close together in breast cancer (MDA-MB-231) cells. Their data shows that in MDA-MB-231 cells Nav1.5 and NHE are found close together in the cell.[72] If the results of this paper are applicable to other forms of cancer, (such as prostate, cervical, lung, and colon cancer) still remains unknown.

My research is the first to my knowledge to show colocalization with vimentin in prostate cancer cells. My research validates the findings of Besson et al. and Bisson et al. and suggests that the proposal of VGSC having a functional role in invadopodia mediated cell invasion may have weight beyond breast cancer and may be applicable to many different types of cancers.

Chapter 5.

Voltage gated sodium channels contribute to invasiveness and metastatic potential in prostate cancer cells

5.1. Introduction

To determine the extent to which VGSC impact prostate cancer cell invasion and potential to metastasis I conducted a comprehensive invasion study using traditional and novel VGSC blockers and a VGSC activator. I used traditional blockers tetrodotoxin (TTX) and lidocaine, channel activator Antillatoxin (ATX), and recently discovered (2018) VGSC inhibitor Cannabidiol (CBD) to explore whether cell invasiveness is compromised in our paradigm and explore VGSC inhibitors and an activator that have yet to be tested. [80]

TTX has been used to show the effects of VGSC inhibition in breast[15], lung[16], prostate[59] cervix[14], ovary[60], as well as in lymphomas[6] and melanomas[6]. Further, Yildirin et al. demonstrated that TTX administration reduces metastasis *in vivo* in rats. [59] Yildirin et al. showed that blocking VGSC in metastatic prostate cancer reduces lung metastasis by > 40% and increases lifespan. [59] TTX completely blocks VGSC,[81] however it is considered a toxin and unsafe for human consumption in high doses. Lidocaine, which reversibly binds to VGSC making it less toxic,[82] is more feasibly used for *in vivo* studies and clinical trials than TTX. Lidocaine is used clinically to numb tissue in a specific area and used to treat ventricular tachycardia. [82] ATX is a VGSC activator[83] and may provide interesting results if invasion is increased when channels are further activated.

CBD, which is commonly used in cancer patients for pain management, may have additional anti-tumorigenic effects such as a reduction in cell invasiveness and metastasis due to an interaction with voltage gated sodium channels. It has been recently found that CBD interacts with Nav1.1-1.7, where it is shown that CBD may bind to and stabilize the inactivated state of the channel. [80] It remains to be seen if CBD has an effect on the endogenously expressed VGSC found in cancer.

Due to the widespread use of CBD for pain management for a multitude of conditions, I can infer that there are few or no harmful side effects to ingestion of this substance. This is of relevance because a likely concern of using VGSC as a therapeutic target for cancer treatment is that these channels are found in neural tissue as well as skeletal and cardiac muscle. Any drug that inhibits these channels could have off target effects in other tissues, such as the brain and heart, especially in higher concentrations. Even in higher concentrations, consumption of CBD has not been listed to have any potentially lethal side effects such as heart attack or stroke. [84]

CBD has been shown to inhibit cancer cell proliferation, adhesion, migration, invasion, and angiogenesis of cancer cells. [84–86] The mechanism by which it does this is currently unknown. VGSC have been associated similarly with cell migration, adhesion and invasion in cancer.[52,59] Thus, I propose that CBD may be producing these anti-tumorigenic effects, at least in part, by interactions with VGSC.

5.2. Methods

Cell culture

I grew all cell lines (ATCC) in their respective mediums supplemented with 10% fetal bovine serum (FBS) at 37C in 5% CO2. PC3 cells uses F-K12 media, LNCaP uses Roswell Park Memorial Institute medium (RPMI) media, DU145 uses Dulbecco's Modified Eagle's Medium (DMEM), All media was filtered as per ATCC recommendations. All media was stored at 4C.

Scratch assay

I seeded cells at 95% confluence in a 6 well plate, at approximately 1.2 x 108 cells per well. Cells were allowed to fully adhere. A 200 uL tip was used to scratch a line down the center of the dish for all wells in each condition. Media was changed in all wells after scratching. Media was supplemented with TTX for the treatment condition. Images were collected at various time points to examine the difference in cell motility.

Invasion assay

Invasion assays were performed in a 12-well-modified Matrigel chamber (Corning® BioCoat™ Matrigel® Invasion Chambers) with a pore diameter of 0.4 µm. Medium supplemented with fetal bovine serum (FBS) was used as a chemoattractant below the chamber. Chambers were hydrated in blank medium (no FBS) for 1 hr. Medium was aspirated out and cell suspension added. A total volume of 500uL of the applied cell suspensions (in blank medium) was placed in each well on the upper part of the chamber at a concentration 2×10^5/ml. Cells were incubated for 24hr at 37°C in 5% CO_2 after the assembly of the chamber to achieve a sufficient number of cells within the pore or just reaching the lower surface of the filter at the termination of the experiment. Chambers were fixed using 4% PFA, stained with Giemsa stain (Sigma-Aldrich) according to accepted protocols on SigmaAldrich.com and imaged under an optical microscope. Images were taken of the chambers and cells were counted. Data is collected as the number of cells that were found imbedded in the gel.

5.3. Results

5.3.1. Voltage-gated sodium channel inhibition reduces cell motility in PC3 cells

As a proof of concept, I conducted several scratch assays to test the hypothesis that VGSC impact the ability of prostate cancer cells to invade into surrounding tissue. (Figure 14). Scratch assays give a crude measure of cell motility and cell migration rates. I compared TTX administration to control conditions.

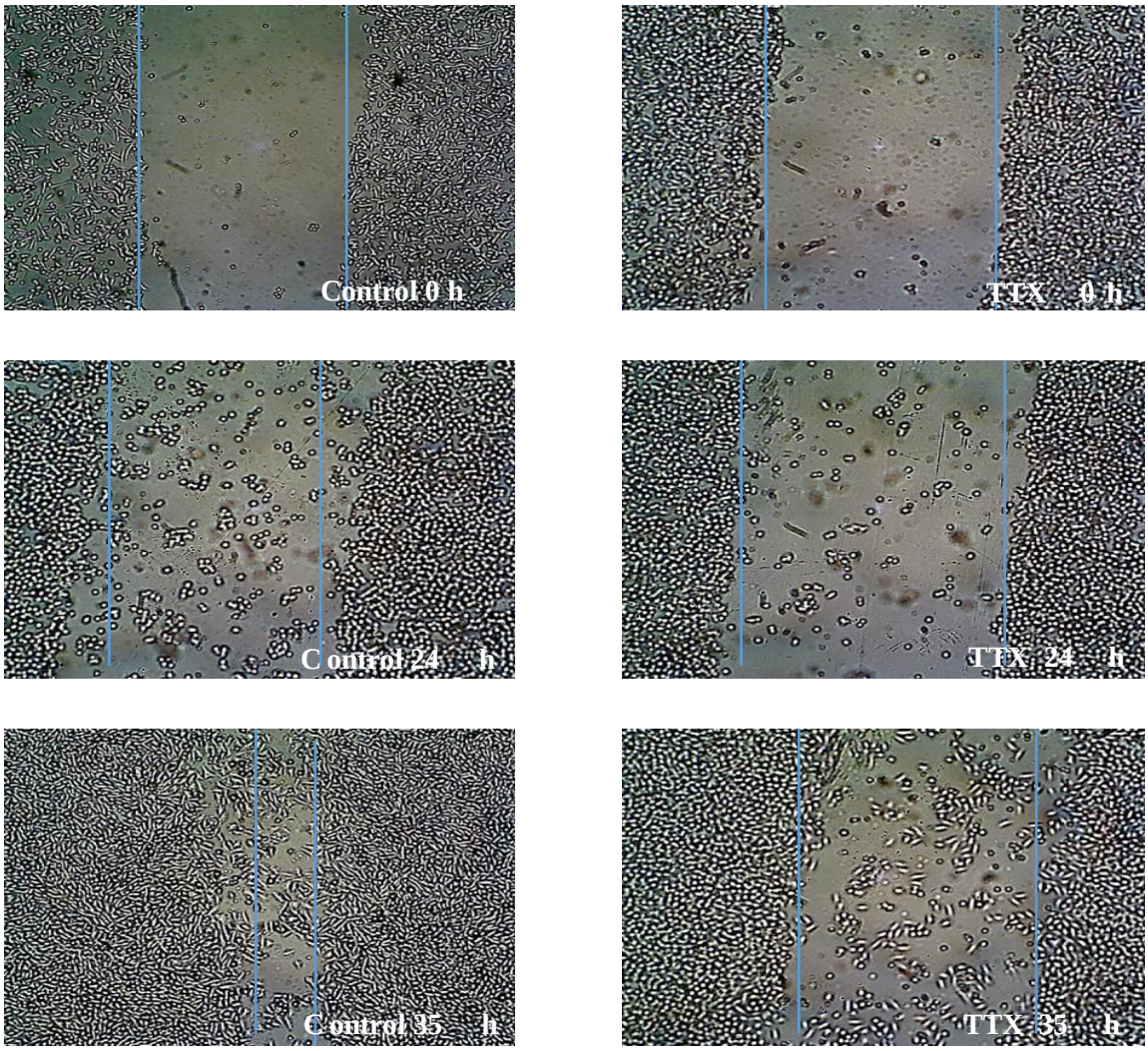

Figure 14. TTX reduces cell motility and cell migration in prostate cancer.
Scratch assay in PC3 cells with the addition of TTX. Left are images of PC3 cells in control conditions, right are images of PC3 cells with addition of TTX. Dishes were imaged at0 hours, 24 hours, 35 hours. The left row and the right row are images of the same dish at different time points. (N=1)

The scratch assays demonstrate that TTX administration reduces cell migration. There is a marked difference in the rate at which cells are able to move in the control condition compared to the TTX. This suggests that TTX impacts the ability of the cancer cell to move in some fashion. Since this is a crude measure, and not as reliable to quantify, I proceeded to complete my invasion study using Matrigel invasion chambers.

Of note is that the scratch assay data was preliminary. Depicted in (Figure 14) is an N=1. I conducted several scratch asssays and found that results were consistent in

that TTX reduced cell motility. I did not formally conduct a series of experiments and conduct statistical analysis as this data was preliminary, and used as a basis for my later experiments.

5.3.2. Voltage-gated sodium channel inhibition reduces invasiveness in prostate cancer cells

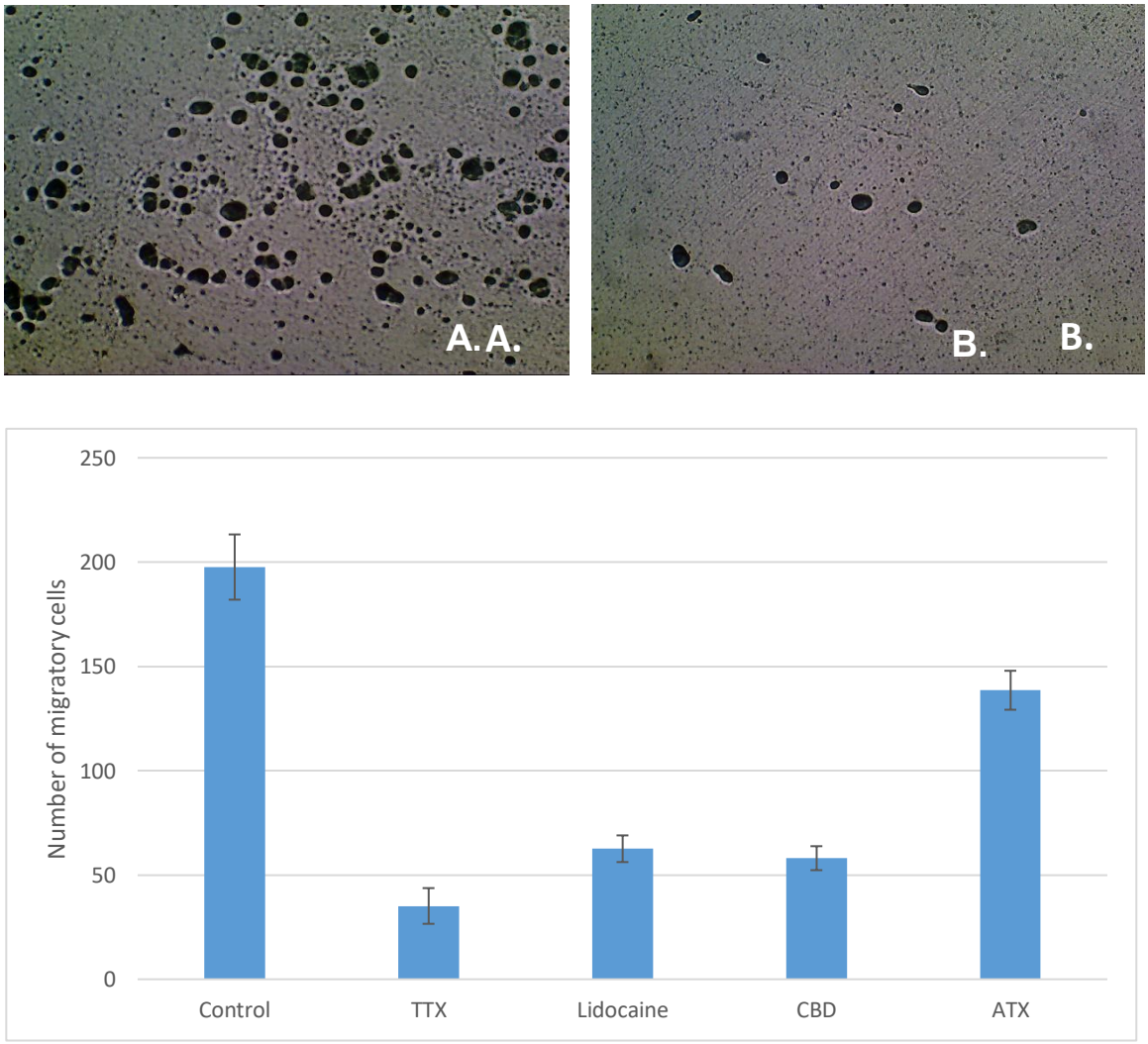

Figure 15. Images from Matrigel chamber experiment in PC3 cells.
Top: Image shows the number of PC3 cells able to migrate in A. control conditions and B. the presence of TTX. Bottom: Invasion assay of the effect of VGSC inhibition or activation in PC3 cells. Data represented as mean number of migratory cells with standard error. (N=12)

I sought to test the hypothesis that VGSC inhibition not only impacts cell migration, but also has an impact on cell invasiveness. To study this I used Matrigel coated chambers specifically designed to test invasiveness in cancer cells. I tested the effects of TTX administration in PC3 cells and found that TTX dramatically reduced cell invasion. (Figure 15). Following the finding that TTX impacts cell invasiveness, I proceeded to test other inhibitors as well as an activator and newly described VGSC inhibitor CBD. I also explored the effect of VGSC inhibition and activation on other metastatic prostate cancer cell lines to gain a comprehensive view of the effects of VGSC in prostate cancer cells. (Figure 15 and Figure 16). N=12 was used for each condition.

TTX was used at a concentration of 1uM. CBD was used at a concentration of 1uM. Lidocaine was used at a concentration of 1mM and ATX was used at a concentration of 1uM. Concentrations were chosen based on the IC50 values of these compounds found in the literature.[87–89] For lidocaine, CBD and TTX I assume a non TTX resistant sodium channel based on the high expression of Nav1.4 and Nav1.6 in both PC3 and LNCaP cells from my Aim 1 data.

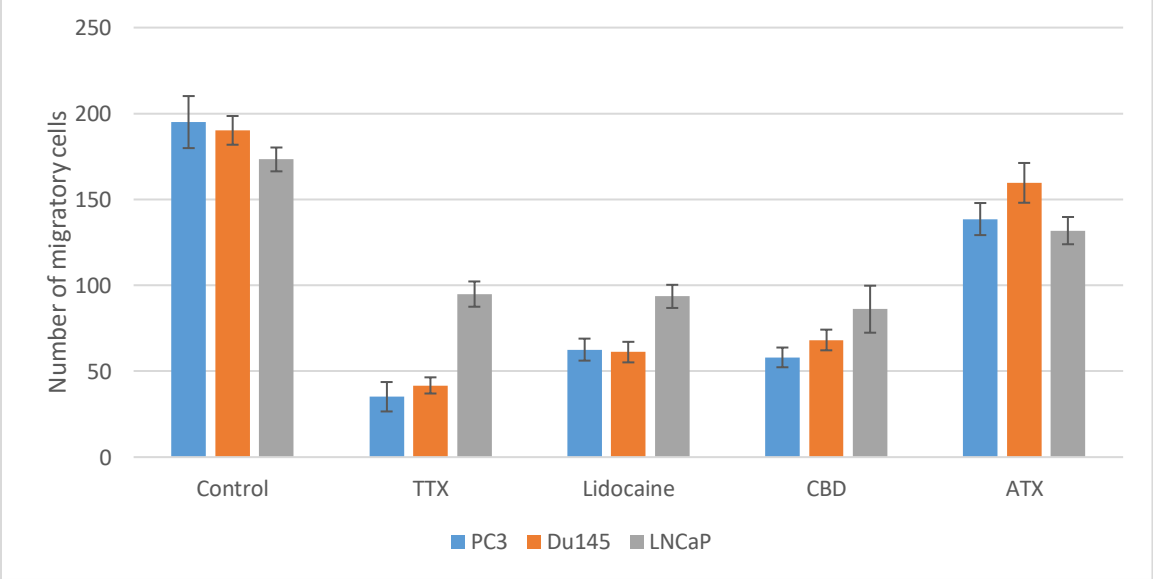

Figure 16. Effects of VGSC inhibition and activation on prostate cancer cell invasion.
Cell lines shown include PC3 cells, DU145 cells, and LNCaP cells. Drugs used include TTX, lidocaine, CBD and ATX at concentrations of 1uM, 1nM, 1uM and 1 uM. Data is represented as mean number of migratory cells with standard error included. N=12 for each condition.

In PC3 cells TTX, Lidocaine and CBD reduce cell invasiveness significantly at P<0.0001. (P<0.05). ATX has an effect on cell invasion, reducing it significantly, but to a much lesser extent at P = 0.0222. In DU145 cells TTX, Lidocaine, CBD, and ATX reduce cell invasiveness significantly at P<0.0001. In LNCaP cells TTX, Lidocaine and CBD all significantly reduce cell invasion at P<0.0001. ATX significantly reduced cell invasion as well, however the P value was much closer to the threshold for significance at P = 0.0175.

Table 1. Summary table of statistical analysis of invasion assays.

Cell line	TTX	Lidocaine	ATX	CBD
PC3	P<0.0001	P<0.0001	P = 0.0222	P<0.0001
DU145	P<0.0001	P<0.0001	P<0.0001	P<0.0001
LNCaP	P<0.0001	P<0.0001	P = 0.0175	P<0.0001

A table of the P values obtained from statistical analysis of cell invasion in different treatment conditions. Treatment conditions are compared to control condition and significance accepted if P<0.05. All conditions of TTX, ATX, Lidocaine and CBD were statistically significant.

This data suggests that ATX does not serve to increase cell invasion whatsoever, but rather may have a small effect on reducing cell invasion. TTX, and Lidocaine significantly reduce cell invasion in all cell lines examined. CBD reduces cancer cell invasion significantly in all cell lines examined, and to a similar extent as TTX and Lidocaine.

5.4. Discussion

VGSC inhibition dramatically impacts cell invasiveness. TTX, lidocaine and CBD supplementation all reduce cell invasion significantly. ATX, as a VGSC activator, interestingly did not increase cell invasiveness compared to the control condition. Rather, ATX appeared to slightly reduce invasiveness. LNCaP cells had a less pronounced effect of VGSC inhibition than PC3 and Du145 cells. This may be unsurprising, as our previous data and western blot experiments suggests that LNCaP cells express VGSC to a lesser extent than do PC3 cells.

There have been several studies examining cell invasion in cancers of various types using TTX. [15,16,40,55,56] Invasion has been studied in several different cancer cell lines (breast cancer primarily) using a combination of invasion chambers and scratch assays. Invasion assays with TTX in prostate cancer have been conducted in rat Mat

Lylu cells and AT-2 cells,[16] as well as in human derived in PC3 cells. [71]Lanadio et al. only conducted studies in PC3 cells and decided against conducting invasion assays in LNCaP cells. Nakajima et al. conducted invasion assays examining PC3 cells and Mat Lylu cells. [90] I am primarily interested in the results found in human derived metastatic prostate cancer lines, of which only PC3 cells have yet been published.

My data confirms and expands upon the existing literature for effects of VGSC inhibitors on prostate cancer cell invasion. I have found that TTX significantly affects PC3 cell invasion in our paradigm, confirming the existing studies that have been conducted by Laniado et al. and Nakajima et al. [71,90] Further, I have expanded my exploration of prostate cancer cells to include LNCaP and Du145 cells to .compare the effects of VGSC inhibition in different metastatic cell lines. An affect in PC3 cells but no effect whatsoever in any other metastatic cell lines is not very promising. Rather, I have shown that the effect of TTX inhibition decreasing cell invasiveness is consistent across several different human derived metastatic prostate cancer cell lines. Mat Lylu cells were not examined as I strove to explore effects of VGSC in human derived metastatic prostate cancer cell types and restricted my search to include Du145 and LNCaP cells as well as PC3 cells. These cell lines are derived from human prostate cancer that has metastasized to the brain supraclavicular lymph node, and bone respectively[62] and provide a more full-picture view of the effectiveness of VGSC inhibition in reducing invasion in prostate cancer cells.

To thoroughly explore the effectiveness of a VGSC based therapeutic approach to metastatic prostate cancer, I sought to test less toxic alternatives and have expanded the knowledge of VGSC inhibitors effective for reducing invasion in prostate cancer cells. TTX provides a complete block of VGSC, offering a clear picture of what occurs in a complete absence of VGSC activity. However, TTX is considered extremely toxic for human consumption and therefore results of TTX administration may not be as applicable to humans. I explored alternate drugs in addition to TTX that have not been explored in the literature including lidocaine, ATX, and CBD. Lidocaine binds reversibly to VGSC and is thus less toxic. [82] Lidocaine is used clinically as an anesthetic and can be used locally at a high concentration without adverse side effects. [82] The finding that lidocaine and CBD are nearly as effective as TTX as an inhibitor of cancer cell invasion may open research opportunities examining non-toxic VGSC inhibitors *in vivo*.

CBD is a newly discovered VGSC inhibitor (2018).[80] CBD significantly reduces cell invasiveness and I think that this may be, at ;least in part, due to its role as a VGSC inhibitor. This is interesting indeed as there is a wealth of literature on the effectiveness of using CBD as an adjuvant therapy for pain management in cancer patients. [84,85] It may be that CBD imparts some advantage besides pain management[85] to cancer treatment, namely an unforeseen effect on VGSC that impacts cancer invasion and metastasis.

CBD may interact with a number of targets, so it is difficult to say whether the decrease in cell invasiveness is due solely to a role in VGSC inhibition. The effects of CBD in the cell are not currently very well understood. These effects may be due to CBD interacting with VGSC, due to interactions with another receptor or another target in the cell, or due to a combination of things. While it is interesting that CBD decreases cell invasion in prostate cancer cells and can act as a VGSC inhibitor, more research is needed to conclude whether CBD impacts cell invasion due to VGSC inhibiton.

My research supports the finding that VGSC inhibition significantly impacts cell invasion and supports the suggestion that VGSC inhibition is likely to reduce metastasis in late stage, metastatic prostate cancer. Cell invasion is the key step crucial for metastasis to occur. Cell movement and degradation of the ECM is needed for cancer cells to intravasate into the blood stream and extravasate to distant tissues. VGSC are most apparent in late stages of the disease such as metastatic, castration resistant or neuroendocrine prostate cancer (Figure 9).

This research contains several limitations. It is possible that the results of this experiment are due to other factors besides VGSC inhibtion. TTX does not affect cell viability,[91] or cytotoxicity. [92] TTX is also highly VGSC specific. [91] These facts were used to support the idea that if a difference in the number of migratory cells was observed, it would likely be due to an affect on VGSC inhibition. However, it remains possible that the changes to number of mean migratory number of cells that were observed, are due to changes in cell proliferation as opposed to VGSC inhibiton. Testing to look for effects on cell proliferation and rule cell proliferation out as a confounding factor were not done. Future directions include testing whether the drugs used in this study have an affect on cell proliferation to rule out confounding factors.

It is interesting that ATX, a channel activator slightly reduced cell invasion. I hypothesized that ATX administration would increase cell invasion by increasing sodium current through sodium channels. It remains possible that these results were due to an unforeseen off target effect of ATX administration. Like TTX, it is possible that ATX has an effect on cell proliferation, which would explain the results. Further testing on whether ATX affects cell proliferation is warranted. ATX activates channels by slowing the process of inactivation[83] and not by decreasing maximum current. This is relevant because it means that in the presence of ATX the amount of sodium ions conducted into the cell is increased, however the amount of VGSC channels that become activated has not changed. If this is so, it is worthwhile to thoroughly examine whether ATX has any off target effects in the cell.

My research has expanded upon the current knowledge of VGSC inhibition on cell invasion and brought the original hypothesis of my thesis to conclusion. Further, the result that CBD is a potent inhibitor of cancer cell invasion and may have this effect due to, at least in part, an effect on VGSC is interesting and may open further research opportunities in the field. This invasion assay shows that the effects of VGSC inhibition are consistent across several metastatic cell lines and explores the effects of alternate VGSC inhibitors and activators such as lidocaine, CBD and ATX. My previous localization study shows that VGSC colocalize with vimentinand the invasion data supports my theory that VGSC play a role in cancer cell invasion by a role in invadopodia. In my original hypothesis I proposed that VGSC containing cancers are more aggressive due to a functional role in invadopodia. I have now shown that functionally, VGSC inhibition impacts cell invasion, and by extension probability of metastasis. It is likely then, that inhibiting VGSC compromises the function of invadopodia which prevents the cell from migrating through tissue microenvironments and degrading the ECM as rapidly. This may serve to explain why VGSC inhibition has the effect is does on cprostate cancer cell invasion.

Chapter 6.

Discussion

6.1. Summary of results

My research demonstrates that i) VGSC are expressed in metastatic prostate cancer cell lines, ii) that VGSC isoforms expressed may differ depending on the cell type, iii) offers the first line of evidence that VGSC localize in invadopodia in prostate cancer, and iv) demonstrates the effects of VGSC inhibition on cancer cell invasion. Collectively, my research adds weight to the theory that VGSC increase cell invasion by a functional role in invadopodia.

6.2. Discussion

While this research has answered the question of what function VGSC serve in prostate cancer, several new questions arise. How is it possible for VGSC to be expressed in a tissue that does not normally express VGSC? What is the mechanism by which VGSC act to aid the function of invadopodia? I will now discuss my theories regarding these two pertinent questions.

I theorize that the reason why cancer cells can spontaneously express ion channels normally only found in excitable tissue has to do with epigenetic dysregulation in cancer and may in part have to do with the predisposition for neuroendocrine cancer cells to express neural and endocrinal proteins.

6.2.1. Epigenetic dysregulation and neuroendocrine differentiation

Cancer cells show extensive reprogramming of epigenetics including DNA methylation, histone modification, nucleosome positioning and microRNA expression. [93–95] Genetic changes are a widely accepted cause of carcinogenesis, where increased cell proliferation and metastatic potential are conveyed by mutations in key genes that regulate the cell cycle. It is now accepted that cancer cells have drastically different

epigenetics compared to somatic cell lines. Cells undergo epigenetic changes both in the initiation of cancer as well as throughout cancer progression. [96] Genes can be silenced, upregulated, or spontaneously expressed by changing DNA methylation patterns or histone packing. [93–95] Therefore, it is possible that VGSC may be able to be spontaneously expressed in tissues that do not normally express VGSC due to drastic changes in epigenetic regulation of cancer cells. More research is needed to say for certain, but it is likely that spontaneous expression of the VGSC genes is the result of alterations in DNA methylation patterns and histone packing to “un-silence” the genes.

Another theory of relevance is that VGSC are found in excitable tissues, and expression may occur as a result of neuroendocrine differentiation in later stages of the disease. It is interesting that VGSC, hugely abundant in neurons, are expressed most highly in later stages of cancers when neuroendocrine differentiation is likely to occur. As cancers become more aggressive the cells can take on features of neurons and endocrine cells that are not present in their tissues of origin. When a cancer cell undergoes neuroendocrine differentiation, the cell accumulates markers that are typically found in neurons.

Neuroendocrine differentiation has been studied to the greatest extent in prostate cancer[10–12,97] but can also occur in other cancers. Cancers such as cervical,[98] breast,[99,100] thymus,[101] small cell lung,[102] and non-small cell lung[102] have also been shown to differentiate into neuroendocrine cells in the last stages of the disease. It is unclear whether VGSC expression is coincidental and unrelated, or whether VGSC expression occurs along with that of other markers of neuroendocrine differentiation. It has not yet been examined if VGSC are present significantly higher in neuroendocrine cancer cells compared to pre-neuroendocrine differentiated cancer cells. It may be that expression of these channels is upregulated along with other neural and endocrine markers as cancer cells undergo neuroendocrine differentiation.

6.2.2. Mechanistic speculations

Sodium entry alone would not explain why cancer cells which express VGSC have increased survivability and invasiveness. Following sodium entry, however, there may be a downstream target that promotes invadopodia function. Sodium gradients drive many energetically unfavorable physiological processes. Examples of transporters

that require a sodium gradient include the sodium hydrogen exchanger (NHE),[79] the sodium calcium exchanger (NCX),[103] the Cl- anion exchanger that operates in parallel with NHE,[104] and sodium glucose transporters SGLT1 and SGLT2 in the small intestine and in the nephron. [105] Of these sodium gradient driven transporters, two seem likely to have an impact in invadopodia; NCX and NHE.

NCX facilitates sodium movement down its concentration gradient and calcium movement in the opposite direction. Normally, sodium is at a higher concentration in the ECM and is transported into the cell, with calcium moved out of the cell. However, NCX can also operate in reverse-mode to bring calcium into the cell. Calcium ions are needed for many physiological processes such as vesicle transport and exocytosis,[106] signal transduction where they act as a secondary messenger,[106] muscle contraction,[107] and is used as a cofactor in many biological reactions. A rapid influx of sodium ions through VGSC might have a downstream effect on NCX, which would alter calcium handling for events such as vesicle exocytosis or signal transduction in invadopodia.

Inward current through VGSC would also sufficiently depolarize the membrane to activate a voltage gated ion channel such as a calcium channel.[108] This can be seen in neural synapses for example, where voltage gated calcium channels are activated by depolarization near the axon terminal and bring in calcium to assist in vesicle docking and release of neurotransmitters into the synaptic cleft.[108]Although voltage gated calcium channels do not require a sodium gradient, they can be activated by membrane depolarization, which occurs near VGSC. This process can occur independently of NCX and would result in a similar increase in intracellular calcium that would alter calcium handling in the cell. In addition, recent studies have found that voltage gated calcium channels are also upregulated in later stages of cancer.[109,110,52] This suggests that upregulation of voltage gated calcium channels could be occurring in parallel with upregulation of VGSC channels. Upregulation of voltage gated calcium channels would have a similar effect on invadopodia to upregulation of NCX.

NHE is another transporter that is directly affected by sodium gradients in a cell. NHE transports sodium down its concentration gradient in exchange for H+ ions transport in the opposite direction. As with the NCX, NHE can also operate in reverse-mode. NHE is responsible for a number of things such as regulation of cell volume and pH,[111] regulation of pH of lysosomes[112] and endosomes,[113] and cell adhesion to the

ECM.[111] Cytoskeletal anchoring of NHE also has indirect effects on migration, cell proliferation, and apoptosis.[111] NHE may play a key role in acidification to assist in ECM degradation, an important property of metastatic cells. NHE aids in acidification of vesicles, which could then be released into the ECM, or could directly acidify the ECM near the leading edge of the cell. Tumor hypoxia induces the expression of NHE in invadopodia in breast cancer cells.[67] NHE also impacts invasiveness by regulation of MMPs[67] and cathepsins.[67] In this scenario, VGSC may bring sodium in, and bring hydrogen ions out of the cell into the ECM. Although this makes sense, it is more likely that acidification of the ECM and secretion of MMP's occurs in a more controlled and regulated fashion, such as vesicle formation.

Sodium permeation through VGSC increases cytoplasmic sodium concentrations relative to the inside of endosomes and may result in Na+ ions entering endosomes, and H+ ions being shuttled into the cytoplasm. This scenario would result in less H+ in endosomes and the cytoplasm becoming acidic, which seems unlikely. The answer must then be more complex than that. Although few studies have been conducted examining whether vesicles are required for MMP release in invadopodia it remains unclear[114–118] It is not generally accepted whether ECM degradation occurs due to vesicle formation and release, or by direct acidification near the plasma membrane.

In endosomal acidification under normal conditions, sodium gradients are used to activate NHE to transport sodium into the vesicle and hydrogen out of the vesicle and into the cytosol .[113] Subsequently, an ATPase proton pump transports H+ ions down their concentration gradient into the vesicle, thus making the contents of the vesicle more acidic. A similar mechanism may occur in cancer cells, which utilise VGSC to drive the activity of NHE and subsequent ATPase proton pump activity to acidify vesicles for subsequent release into ECM. In either the case of NHE activity on the plasma membrane, or in vesicle release, it remains possible that VGSC may drive this activity.

A study by Brisson et al. is the first to add credibility to the theory that VGSC are localized in invadopodia. In this study, it was shown that Nav1.5 co-localizes with NHE-1 sodium hydrogen exchanger in invadopodia in breast cancer cells.[51] NHE-1, caveolin-1 and Nav1.5 co- immune-precipitated, which suggests that these proteins co-localize. [51] Although VGSC and NHE-1 transporters co-localize, the nature of their relationship has yet to be elucidated.

Finally, VGSC β subunits interact with both cell adhesion molecules (CAMs) and ECM proteins for cell anchoring and may also play a role in cell motility and survivability in cancer cells.[34] VGSC interactions with the ECM and CAMs may help cells detach from their original location and migrate more easily through the ECM. [34] Cells expressing VGSC are less contact-dependent than cells which express none. [34] β subunits can act as signalling molecules and interact with CAMs such as neurofascin and contactin, as well as molecules found in the ECM including tenascin.[34] VGSC β subunit interactions with CAMs and ECM proteins may allow cells expressing VGSC channels to form new interactions with the cytoskeleton and surrounding environment. As such, VGSC β subunits may assist in migration through tissue microenvironments which could be further advantageous for cancer cells.

6.3. Future directions

Further avenues of research include examining potential downstream targets of VGSC activation such as voltage-gated calcium channels, NHE, and NCX as well as testing VGSC CRISPR knockout cells to fully flesh out the mechanism by which VGSC increase functionality of invadopodia in cancer cells. VGSC proposed downstream targets are summarized in (Figure 17).

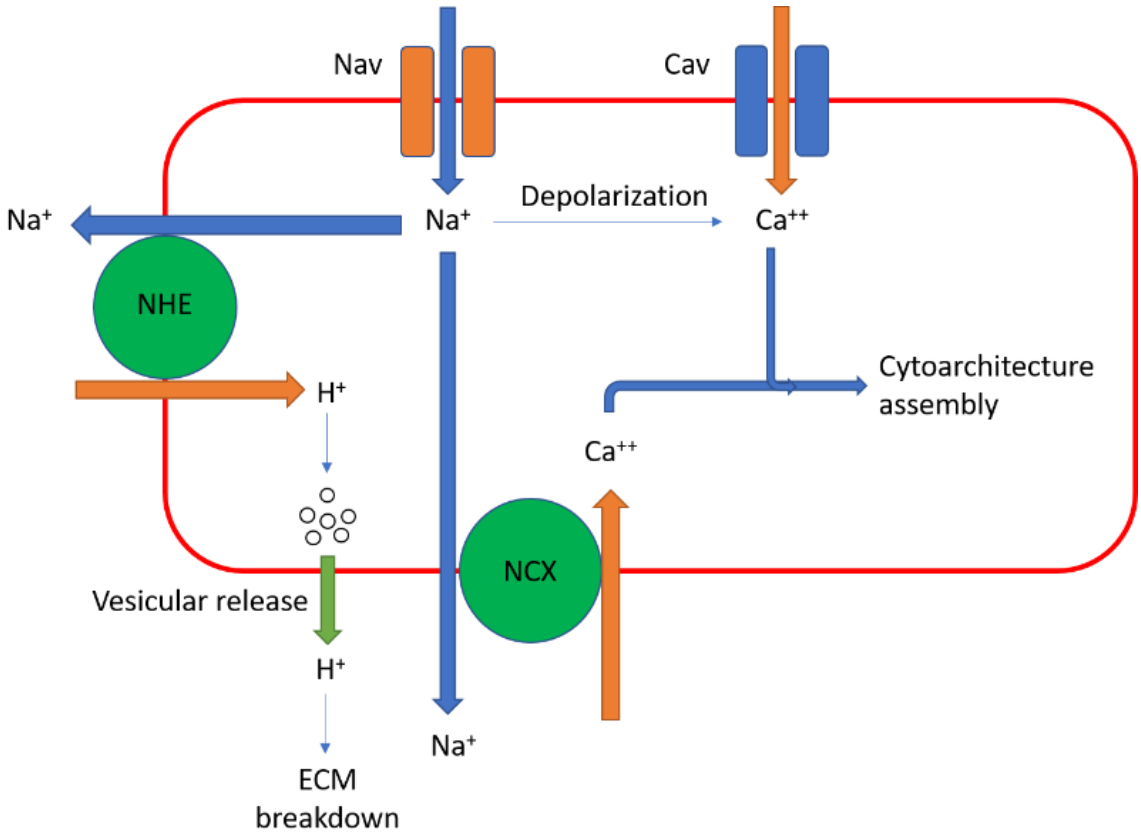

Figure 17. Hypothesis for mechanisms by which VGSC increase invasiveness in cancer cells.

This schematic summarizes potential downstream targets of VGSC.Sodium is a driving force for many transporters and exchangers, most notably NCX and NHE. VGSC will depolarize the membrane sufficiently to activate other voltage gated ion channels such as voltage gated calcium channels. VGSC can thus affect hydrogen ion exchange and calcium handling which has functional consequences for invadopodia.

I have taken several steps down each avenue and will now present my preliminary findings for further avenues of research. I have generated CRIPSR knockout lines to test the hypothesis that VGSC play a pivotal role in the function of invadopodia (Figure 18-19). I wanted to conduct invasion experiments to determine whether knocking out VGSC produces the same effect as VGSC inhibition.

I have conducted invasion assays using different knockout colonies and presented my findings below. To publish these findings, further testing should be done to generate a higher n number. Currently I have presented my invasion findings with an N=4 for each KO line. My preliminary data is promising, however, it would need to be expanded upon to draw any real conclusions.

Further, it would be interesting to quantify invadopodia formation microscopically and explore whether formation is reduced or inhibited in the presence of TTX, or in a VGSC knockout line. This may provide further credibility to the theory that VGSC play a functional role in invadopodia.

Robert Payer from Dr. Tim Beischlag's lab generated the CRISPR KO plasmids for transfection. Robert designed the CRISPR primers, and did the bacterial work to generate the plasmids. He was also available for advice and help during the transfection, colony selection process and western blots to test the knockout colonies. Dr. Tim Beischlag provided the reagents and equipment necessary for the transfection and colony selection process as well as the western blots to check for the success of a knockout.

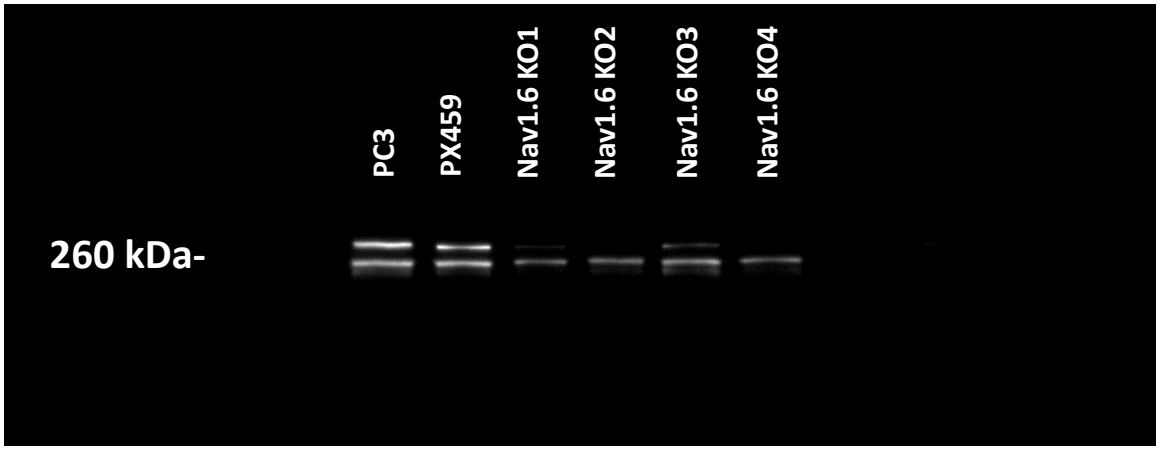

Figure 18. Western blot of Nav1.6 in CRISPR knockout.
The left two gel columns contain control PC3 cells (leftmost) and PX459 cells (vehicular control cells). The other wells contain different colony selections for CRISPR Nav1.6 kncokouts in PC3 cells. The second lower band denotes a secondary splice site, however, the absence of the top band in clear in nearly every colony selection tested.

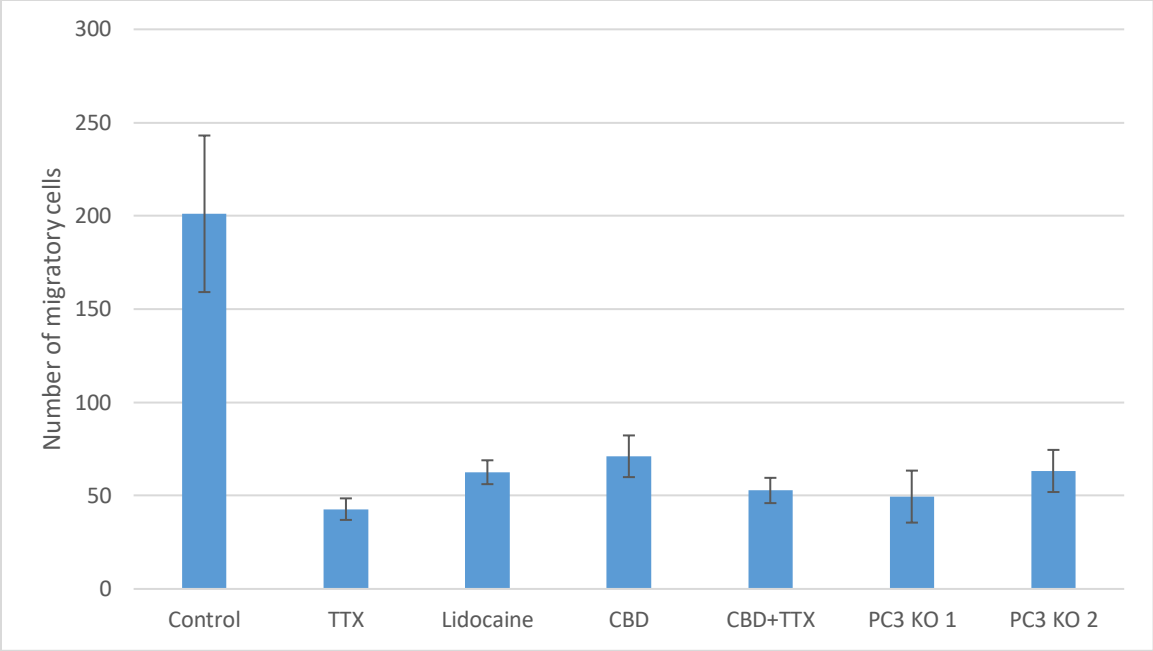

Figure 19. Knocking out Nav1.6 reduces cell invasion in PC3 cells.
CRISPR knockouts of Nav1.6 were tested and results compared to control PC3 cells and PC3 cells with added VGSC inhibitors. PC3 KO1 and PC3 KO 2 denote two separate KO lines generated from PC3 cells. KO lines are compared to control, TTX, Lidocaine, CBD, and CBD+TTX conditions. Data represented as number of migratory cells. Standard error bars included. N=8 for Control, TTX, Lidocaine, CBD and CBD+TTX conditions. Preliminary data from KO lines represented as N=4.

I also conducted some preliminary experiments to explore whether NCX, Cav3.2, or NHE are potential downstream targets of VGSC activity. qPCR shows that NHE and NCX expressed along with Nav1.6 in PC3 cell. (Figure 20). Some preliminary tests were conducted to look for the presence of Cav3.2, a voltage-gated calcium channel, however no trace of Cav3.2 was found. Data was collected as a triplicate (N=3) from the same sample of PC3 cells.

Experiment was repeated several times and presence of NCX and NHE alongside Nav1.6 in PC3 cells was consistent across different qPCR readouts. Each experiment was run as a triplicate. Figure only represents data from one experiment.

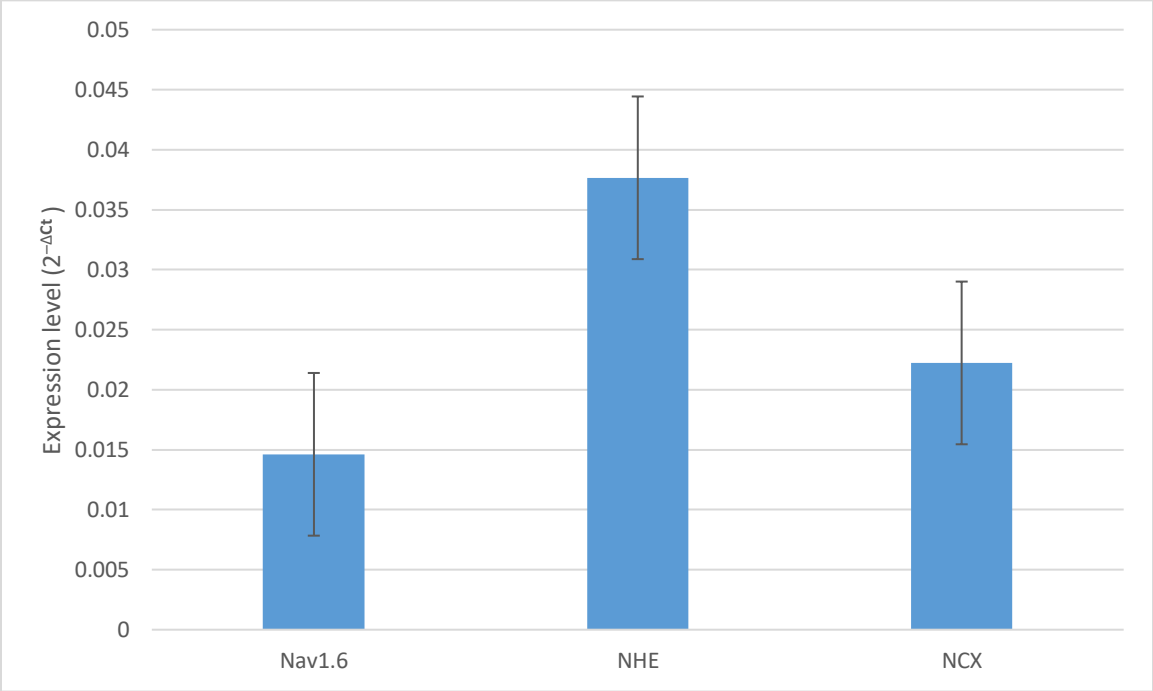

Figure 20. NCX and NHE are expressed in PC3 cells while Cav3.2 is not.
NHE and NCX are also expressed in PC3 cells alongside Nav1.6. Expression is represented as $2^{-\Delta Ct}$ values.

I also conducted several imaging experiments to examine colocalization between NCX and NHE, our believed two strong potential downstream targets of VGSC. Here are the preliminary figures I generated. (Figure 21-23)

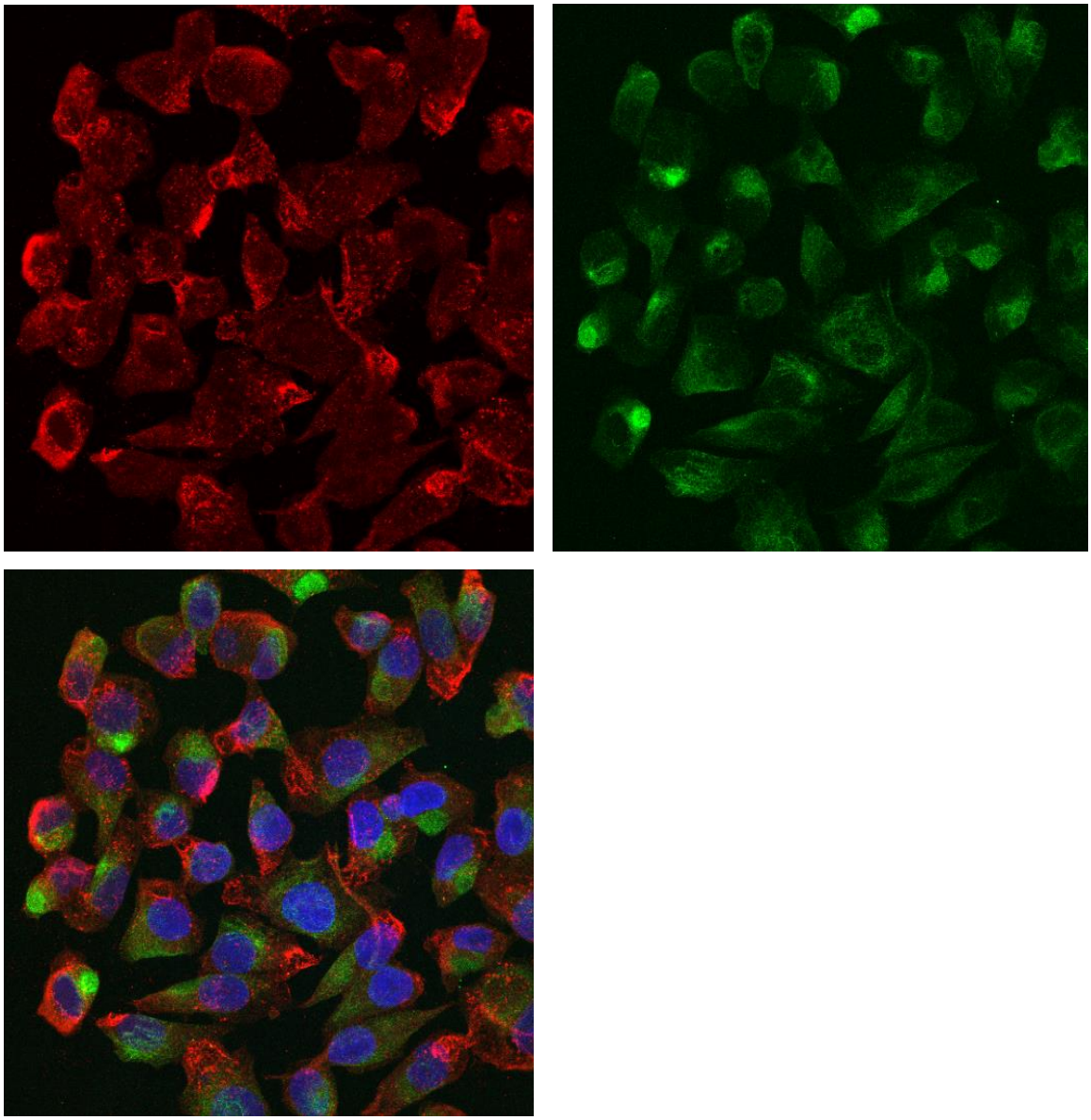

Figure 21. NHE does not appear to colocalize with Nav1.6 in PC3 cells.
NHE (red) and Nav1.6 (green) in PC3 cells. Hoescht nuclear stain in blue. NHE appears to concentrate in a different part of the cell compared to Nav1.6.

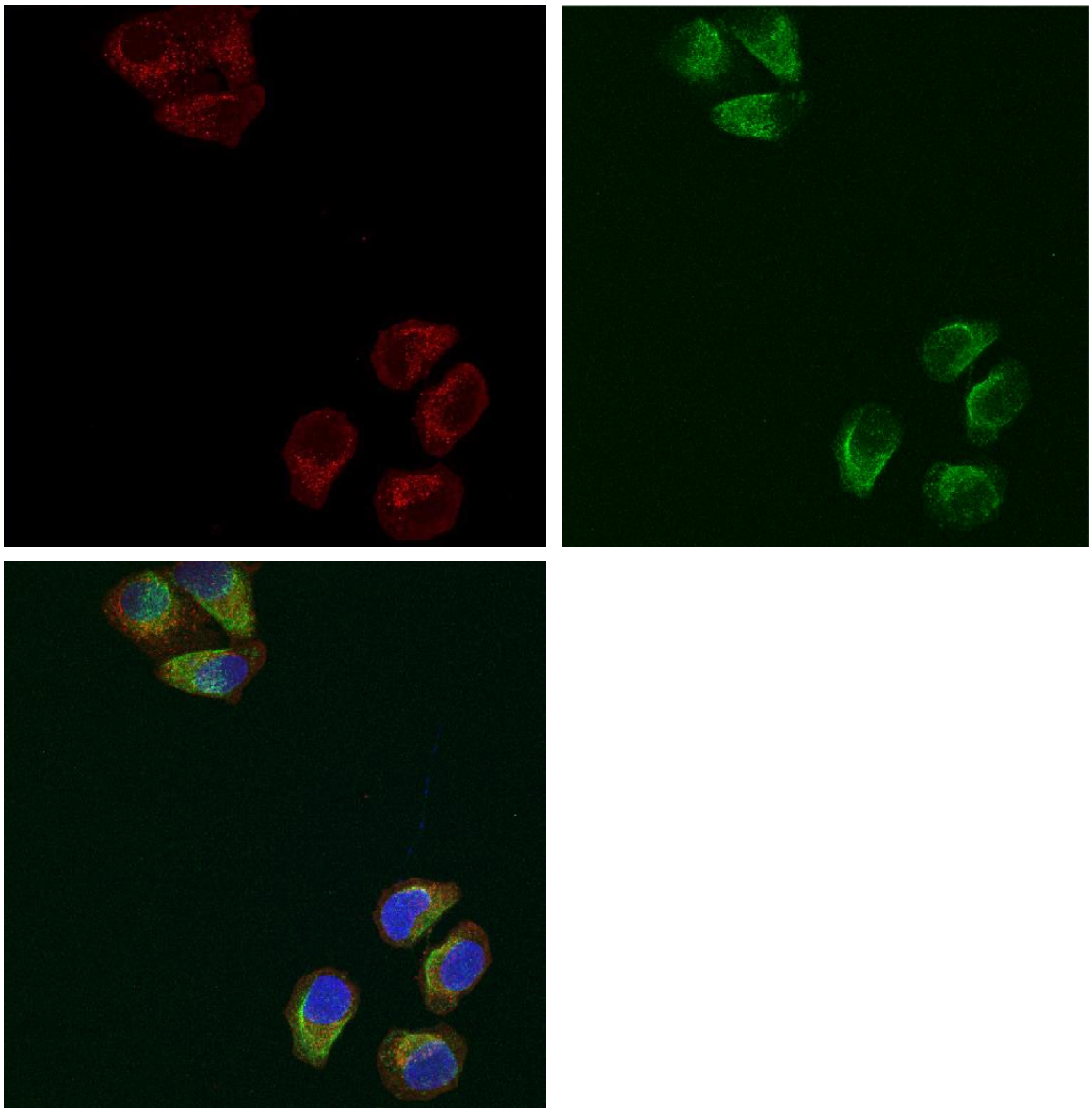

Figure 22. NCX and Nav1.6 appear to colocalize in PC3 cells.
NCX (red) and Nav1.6 (green) in PC3 cells. Hoescht nuclear stain in blue. NCX appears to be found in similar areas of the cell to Nav1.6.

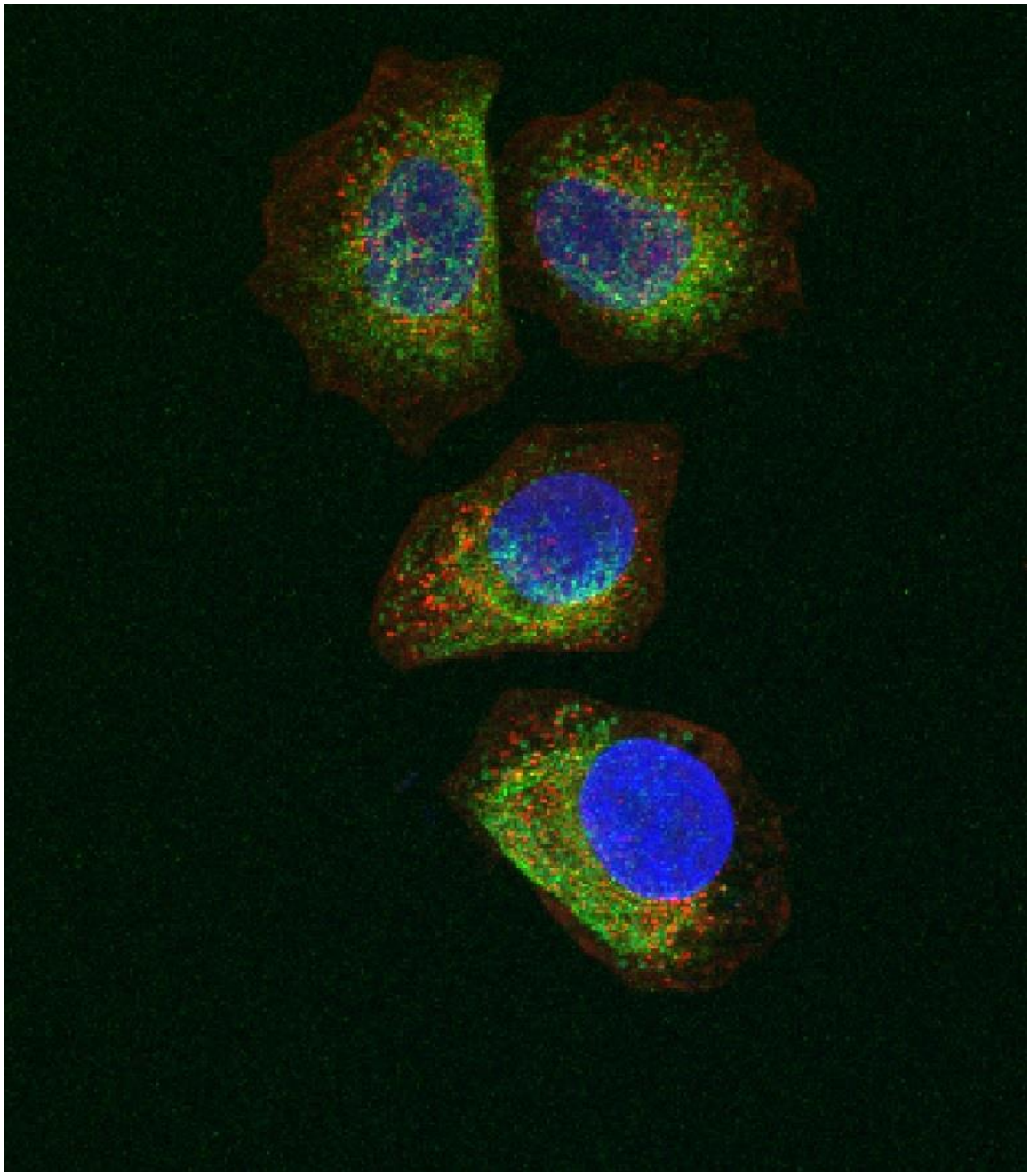

Figure 23. Close up of NCX and Nav1.6 in PC3 cells.
NCX (red), Nav1.6 (green), and Hoescht nuclear stain in blue. Nav1.6 and NCX appear to localize in the same area of the cell.

I should note that these figures are preliminary and further data should be collected prior to making conclusive statements. However, based on the preliminary images of NHE and NCX expression it would appear that NHE expression might not follow Nav1.6 expression, and that NCX may be situated in a similar part of the cell. As to the degree of colocalization, further testing is required.

NHE is reported in the literature to strongly colocalize with VGSC [51] however our data does not support this. Granted, NHE and VGSC colocalization was reported in breast cancer cells, [51] and these images are generated from a prostate cancer cell line. My results may differ due to the cancer type and cell line examined. It is intriguing, however, that NHE expression does not appear to match Nav1.6 expression in PC3 cells. It may be interesting to conduct the same experiment in different prostate cancer cell lines to determine whether results are consistent.

NCX on the lower magnification on the fluorescent microscope shows what appears to be strong colocalization between Nav1.6 and NCX ((Figure 20). Further, a close up of the 60x oil magnification revealed that both VGSC and NCX are concentrated into ball like structures, which appear as though they could be vesicles in the leading edge of the cell. More testing is required to say for certain. (Figure 23). More data should be collected, and statistical analysis run to examine whether NCX colocalizes with VGSC.

I conducted a preliminary check on NCX colocaliztion and found a strong colocalization between NCX and Nav1.6. I collected a Pearson correlation coefficient of 0.89 for N=29 cells. This yields a p value of <0.0001 ($p<0.05$) and suggests a high colocalization. Limitations of this preliminary testing include that only slides fixed and stained on the same day were used for data collection. Therefore, to be more certain of findings cells should be fixed and stained several more times to determine whether results are consistent.

More research is needed to make conclusive statements on NCX and NHE localization in prostate cancer cells. It also may be of interest to examine the effect of blockers for NHE and NCX in the presence and absence of TTX determine whether blocking NHE or NCX produces the same effect as blocking VGSC.

6.4. Conclusion

Firstly, I demonstrated that VGSC isoforms are not consistent across cell types and demonstrated that VGSC expressed in prostate cancer display typical voltage-gated ion channel properties. Secondly, I demonstrated that VGSC localization is clustered in the leading edge of the cell and colocalizes with vimentin and is suggested to be found in or near invadopodia in cells. Thirdly, I showed that VGSC inhibition has significant consequences on reducing cancer cell invasion. Finally, I demonstrated preliminary results for testing NCX and NHE as downstream targets of VGSC activity. Collectively, my data suggests that VGSC activity is important in cancer cell invasion due to a functional role in invadopodia and VGSC may have promise as a therapeutic target for reducing invasiveness and probability of metastasis in prostate cancer.

My original hypothesis was that VGSC increase invasiveness in prostate cancer cells by a functional role in invadopodia. I have demonstrated colocalization data that suggests that VGSC localize in invadopodia and provided evidence that VGSC inhibition has consequences on cell invasion.

VGSC inhibition has consequences for metastatic potential and reducing cancer metastasis *in vivo* and future testing is warranted to test the potential of a VGSC based therapeutic approach in prostate cancer. Yildirim et al. demonstrated that VGSC inhibition through low concentrations of TTX reduced lung metastasis in prostate cancer by 40% in rats. [59] . Further VGSC inhibitor studies in animal models[59] may be warranted to determine the extent to which VGSC inhibition impacts metastatic potential. However, the extent to which cell invasiveness is reduced *in vitro* is promising. Even less potent inhibitors such as lidocaine and CBD, VGSC inhibition has demonstrated a surprisingly significant decrease in cell invasion. VGSC based therapies may prove to be a neat way to prevent the formation of invadopodial structures.

The preliminary data I have generated for further avenues of research shows interesting results. More data collection is needed to be certain of findings regarding my preliminary data on NHE and NCX, however, it appears that NHE may not be the

downstream target of VGSC activity as previously thought. [72] As well, NCX may be an interesting unforeseen downstream target of VGSC activity.

My research has added weight to the theory of VGSC dependent invadopodia. My research may open further research opportunities such as exploring the consequences of a VGSC CRISPR knockout and exploring potential downstream targets of VGSC activation such as NCX and NHE. My research may open future research opportunities and show potential for a VGSC based therapeutic approach in prostate cancer.

References

1. Siegel R, Naishadham D, Jemal A. Cancer statistics, 2013. *CA Cancer J Clin*. 2013;63(1):11-30. doi:10.3322/caac.21166

2. Hamidi H, Ivaska J. Every step of the way: integrins in cancer progression and metastasis. *Nat Rev Cancer*. 2018;18(9):533-548. doi:10.1038/s41568-018-0038-z

3. Siegel R, Naishadham D, Jemal A. Cancer statistics, 2013. *CA Cancer J Clin*. 2013;63(1):11-30. doi:10.3322/caac.21166

4. Nuttall R, Bryan S, Dale D, et al. Canadian Cancer Statistics 2017. *Can Cancer Soc*. 2017. http://www.cancer.ca/~/media/cancer.ca/CW/publications/Canadian Cancer Statistics/Canadian-Cancer-Statistics-2017-EN.pdf. Accessed November 25, 2017.

5. Wilt TJ, MacDonald R, Rutks I, Shamliyan TA, Taylor BC, Kane RL. Systematic Review: Comparative Effectiveness and Harms of Treatments for Clinically Localized Prostate Cancer. *Ann Intern Med*. 2008;148(6):435. doi:10.7326/0003-4819-148-6-200803180-00209

6. Lin GA, Aaronson DS, Knight SJ, Carroll PR, Dudley RA. Patient Decision Aids for Prostate Cancer Treatment: A Systematic Review of the Literature. *CA Cancer J Clin*. 2009;59(6):379-390. doi:10.3322/caac.20039

7. Dall'Era MA, Albertsen PC, Bangma C, et al. Active Surveillance for Prostate Cancer: A Systematic Review of the Literature. *Eur Urol*. 2012;62(6):976-983. doi:10.1016/J.EURURO.2012.05.072

8. Kirby M, Hirst C, Crawford ED. Characterising the castration-resistant prostate cancer population: A systematic review. *Int J Clin Pract*. 2011;65(11):1180-1192. doi:10.1111/j.1742-1241.2011.02799.x

9. Gupta K, Gupta S. Neuroendocrine differentiation in prostate cancer: Key epigenetic players. *Transl Cancer Res*. 2017;6:S104-S108. doi:10.21037/tcr.2017.01.20

10. Beltran H, Tagawa ST, Park K, et al. Challenges in recognizing treatment-related neuroendocrine prostate cancer. *J Clin Oncol*. 2012;30(36):e386-9. doi:10.1200/JCO.2011.41.5166

11. Aprikian AG, Cordon-Cardo C, Fair WR, Reuter VE. Characterization of neuroendocrine differentiation in human benign prostate and prostatic adenocarcinoma. *Cancer*. 1993;71(12):3952-3965. http://www.ncbi.nlm.nih.gov/pubmed/7685237. Accessed October 12, 2018.

12. Parimi V, Goyal R, Poropatich K, Yang XJ. Neuroendocrine differentiation of prostate cancer: a review. *Am J Clin Exp Urol*. 2014;2(4):273-285. http://www.ncbi.nlm.nih.gov/pubmed/25606573. Accessed October 12, 2018.

13. Brackenbury WJ. Voltage-gated sodium channels and metastatic disease. *Channels (Austin)*. 2012;6(5):352-361. doi:10.4161/chan.21910

14. Hernandez-Plata E, Ortiz CS, Marquina-Castillo B, et al. Overexpression of NaV 1.6 channels is associated with the invasion capacity of human cervical cancer. *Int J cancer*. 2012;130(9):2013-2023. doi:10.1002/ijc.26210

15. Fraser SP, Diss JKJ, Chioni A-M, et al. Voltage-gated sodium channel expression and potentiation of human breast cancer metastasis. *Clin Cancer Res*. 2005;11(15):5381-5389. doi:10.1158/1078-0432.CCR-05-0327

16. Gillet L, Roger S, Besson P, et al. Voltage-gated Sodium Channel Activity Promotes Cysteine Cathepsin-dependent Invasiveness and Colony Growth of Human Cancer Cells. *J Biol Chem*. 2009;284(13):8680-8691. doi:10.1074/jbc.M806891200

17. Fraser SP, Ozerlat-Gunduz I, Brackenbury WJ, et al. Regulation of voltage-gated sodium channel expression in cancer: hormones, growth factors and auto-regulation. *Philos Trans R Soc London B Biol Sci*. 2014;369(1638).

18. Djamgoz MBA, Fraser SP, Ozerlat-Gunduz I, et al. Regulation of voltage-gated sodium channel expression in cancer: hormones, growth factors and auto-regulation. doi:10.1098/rstb.2013.0105

19. Vincent C, Siddiqui TA, Schlichter LC. Podosomes in migrating microglia: components and matrix degradation. *J Neuroinflammation*. 2012;9:190. doi:10.1186/1742-2094-9-190

20. Black JA, Liu S, Waxman SG. Sodium channel activity modulates multiple functions in microglia. *Glia*. 2009;57(10):1072-1081. doi:10.1002/glia.20830

21. Carrithers MD, Dib-Hajj S, Carrithers LM, et al. Expression of the voltage-gated sodium channel NaV1.5 in the macrophage late endosome regulates endosomal acidification. *J Immunol*. 2007;178(12):7822-7832. http://www.ncbi.nlm.nih.gov/pubmed/17548620. Accessed October 28, 2016.

22. Craner MJ, Damarjian TG, Liu S, et al. Sodium channels contribute to microglia/macrophage activation and function in EAE and MS. *Glia*. 2005;49(2):220-229. doi:10.1002/glia.20112

23. Kwong K, Carr MJ. Voltage-gated sodium channels. *Curr Opin Pharmacol*. 2015;22:131-139. doi:10.1016/J.COPH.2015.04.007

24. Catterall WA. From Ionic Currents to Molecular Mechanisms: The Structure and

Function of Voltage-Gated Sodium Channels. *Neuron*. 2000;26(1):13-25. doi:10.1016/S0896-6273(00)81133-2

25. Peters C, Rosch RE, Hughes E, Ruben PC. Temperature-dependent changes in neuronal dynamics in a patient with an SCN1A mutation and hyperthermia induced seizures. *Sci Rep*. 2016;6. doi:10.1038/srep31879

26. Ulbricht W. Sodium channel inactivation: molecular determinants and modulation. *Physiol Rev*. 2005;85(4):1271-1301. doi:10.1152/physrev.00024.2004

27. Guy HR, Seetharamulu P. Molecular model of the action potential sodium channel. *Proc Natl Acad Sci U S A*. 1986;83(2):508-512. http://www.ncbi.nlm.nih.gov/pubmed/2417247. Accessed October 28, 2016.

28. Lipkind GM, Fozzard HA. Voltage-gated Na channel selectivity: the role of the conserved domain III lysine residue. *J Gen Physiol*. 2008;131(6):523-529. doi:10.1085/jgp.200809991

29. Bezanilla F, Armstrong CM. Inactivation of the sodium channel. I. Sodium current experiments. *J Gen Physiol*. 1977;70(5):549-566. http://www.ncbi.nlm.nih.gov/pubmed/591911. Accessed November 2, 2016.

30. Eaholtz G, Scheuer T, Catterall WA, et al. Restoration of inactivation and block of open sodium channels by an inactivation gate peptide. *Neuron*. 1994;12(5):1041-1048. doi:10.1016/0896-6273(94)90312-3

31. Ruben PC, ed. *Voltage Gated Sodium Channels*. Vol 221. Berlin, Heidelberg: Springer Berlin Heidelberg; 2014. doi:10.1007/978-3-642-41588-3

32. Stühmer W, Conti F, Suzuki H, et al. Structural parts involved in activation and inactivation of the sodium channel. *Nature*. 1989;339(6226):597-603. doi:10.1038/339597a0

33. Vilin YY, Ruben PC. Slow Inactivation in Voltage-Gated Sodium Channels: Molecular Substrates and Contributions to Channelopathies. *Cell Biochem Biophys*. 2001;35(2):171-190. doi:10.1385/CBB:35:2:171

34. Isom LL. Sodium channel beta subunits: anything but auxiliary. *Neuroscientist*. 2001;7(1):42-54. doi:10.1177/107385840100700108

35. Pan X, Li Z, Zhou Q, et al. Structure of the human voltage-gated sodium channel Na v 1.4 in complex with β1. *Science (80-)*. 2018;362(6412). doi:10.1126/science.aau2486

36. Barres BA, Chun LL, Corey DP. Ion channel expression by white matter glia: I. Type 2 astrocytes and oligodendrocytes. *Glia*. 1988;1(1):10-30. doi:10.1002/glia.440010104

37. Kaplan MR, Meyer-Franke A, Lambert S, et al. Induction of sodium channel clustering by oligodendrocytes. *Nature*. 1997;386(6626):724-728. doi:10.1038/386724a0

38. Shrager P, Chiu SY, Ritchie JM. Voltage-dependent sodium and potassium channels in mammalian cultured Schwann cells. *Proc Natl Acad Sci U S A*. 1985;82(3):948-952. http://www.ncbi.nlm.nih.gov/pubmed/2579384. Accessed October 28, 2016.

39. Kis-Toth K, Hajdu P, Bacskai I, et al. Voltage-gated sodium channel Nav1.7 maintains the membrane potential and regulates the activation and chemokine-induced migration of a monocyte-derived dendritic cell subset. *J Immunol*. 2011;187(3):1273-1280. doi:10.4049/jimmunol.1003345

40. Black JA, Waxman SG, Allard B, et al. Noncanonical roles of voltage-gated sodium channels. *Neuron*. 2013;80(2):280-291. doi:10.1016/j.neuron.2013.09.012

41. Sontheimer H, Fernandez-Marques E, Ullrich N, Pappas CA, Waxman SG. Astrocyte Na+ channels are required for maintenance of Na+/K(+)-ATPase activity. *J Neurosci*. 1994;14(5 Pt 1):2464-2475. doi:10.1523/JNEUROSCI.14-05-02464.1994

42. Pressel DM, Misler S. Role of voltage-dependent ionic currents in coupling glucose stimulation to insulin secretion in canine pancreatic islet B-cells. *J Membr Biol*. 1991;124(3):239-253. http://www.ncbi.nlm.nih.gov/pubmed/1787535. Accessed March 4, 2019.

43. Braun M, Ramracheya R, Bengtsson M, et al. Voltage-Gated Ion Channels in Human Pancreatic -Cells: Electrophysiological Characterization and Role in Insulin Secretion. *Diabetes*. 2008;57(6):1618-1628. doi:10.2337/db07-0991

44. Carrithers MD, Chatterjee G, Carrithers LM, et al. Regulation of podosome formation in macrophages by a splice variant of the sodium channel SCN8A. *J Biol Chem*. 2009;284(12):8114-8126. doi:10.1074/jbc.M801892200

45. Oppenheimer SB. Cellular basis of cancer metastasis: A review of fundamentals and new advances. *Acta Histochem*. 2006;108(5):327-334. doi:10.1016/j.acthis.2006.03.008

46. Lohmer LL, Kelley LC, Hagedorn EJ, Sherwood DR. Invadopodia and basement membrane invasion in vivo. *Cell Adh Migr*. 2014;8(3):246-255. doi:10.4161/CAM.28406

47. Murphy DA, Courtneidge SA. The “ins” and “outs” of podosomes and invadopodia: characteristics, formation and function. *Nat Rev Mol Cell Biol*. 2011;12(7):413-426. doi:10.1038/nrm3141

48. Linder S, Chen WT, Burgstaller G, et al. The matrix corroded: podosomes and invadopodia in extracellular matrix degradation. *Trends Cell Biol*. 2007;17(3):107-

117. doi:10.1016/j.tcb.2007.01.002

49. Goto T, Maeda H, Tanaka T. A selective inhibitor of matrix metalloproteinases inhibits the migration of isolated osteoclasts by increasing the life span of podosomes. *J Bone Miner Metab*. 2002;20(2):98-105. doi:10.1007/s007740200013

50. Seals DF, Courtneidge SA. The ADAMs family of metalloproteases: multidomain proteins with multiple functions. *Genes Dev*. 2003;17(1):7-30. doi:10.1101/gad.1039703

51. Brisson L, Gillet L, Calaghan S, et al. NaV1.5 enhances breast cancer cell invasiveness by increasing NHE1-dependent H+ efflux in caveolae. *Oncogene*. 2011;30(17):2070-2076. doi:10.1038/onc.2010.574

52. Brackenbury WJ. Voltage-gated sodium channels and metastatic disease. *Channels (Austin)*. 2012;6(5):352-361. doi:10.4161/chan.21910

53. Onkal R, Djamgoz MBA. Molecular pharmacology of voltage-gated sodium channel expression in metastatic disease: Clinical potential of neonatal Nav1.5 in breast cancer. *Eur J Pharmacol*. 2009;625(1-3):206-219. doi:10.1016/j.ejphar.2009.08.040

54. Fraser SP, Salvador V, Manning EA, et al. Contribution of functional voltage-gated Na+ channel expression to cell behaviors involved in the metastatic cascade in rat prostate cancer: I. Lateral motility. *J Cell Physiol*. 2003;195(3):479-487. doi:10.1002/jcp.10312

55. Yang M, Kozminski DJ, Wold LA, et al. Therapeutic potential for phenytoin: targeting Nav1.5 sodium channels to reduce migration and invasion in metastatic breast cancer. *Breast Cancer Res Treat*. 2012;134(2):603-615. doi:10.1007/s10549-012-2102-9

56. Mycielska ME, Fraser SP, Szatkowski M, Djamgoz MBA. Contribution of functional voltage-gated Na+ channel expression to cell behaviors involved in the metastatic cascade in rat prostate cancer: II. Secretory membrane activity. *J Cell Physiol*. 2003;195(3):461-469. doi:10.1002/jcp.10265

57. Roger S, Besson P, Le Guennec J-Y. Involvement of a novel fast inward sodium current in the invasion capacity of a breast cancer cell line. *Biochim Biophys Acta - Biomembr*. 2003;1616(2):107-111. doi:10.1016/J.BBAMEM.2003.07.001

58. Bennett ES, Smith BA, Harper JM. Voltage-gated Na + channels confer invasive properties on human prostate cancer cells. *Pflgers Arch Eur J Physiol*. 2004;447(6):908-914. doi:10.1007/s00424-003-1205-x

59. Yildirim S, Altun S, Gumushan H, Patel A, Djamgoz MBA. Voltage-gated sodium channel activity promotes prostate cancer metastasis in vivo. *Cancer Lett*. 2012;323(1):58-61. doi:10.1016/J.CANLET.2012.03.036

60. Wang R, Shen Y, Cai J, Lei M, Wang Z. Expression of voltage-gated sodium channel α subunit in human ovarian cancer. *Oncol Rep*. 2010;23(5):1293-1299. doi:10.3892/or_00000763

61. Suy S, Hansen TP, Auto HD, et al. Expression of Voltage-Gated Sodium Channel Nav1.8 in Human Prostate Cancer is Associated with High Histological Grade. *J Clin Exp Oncol*. 2012;1(2). doi:10.4172/2324-9110.1000102

62. Cunningham D, You Z. In vitro and in vivo model systems used in prostate cancer research. *J Biol Methods*. 2015;2(1):17. doi:10.14440/jbm.2015.63

63. Brambilla E, Moro D, Gazzeri S, Brambilla C. Alterations of expression of Rb, p16INK4A and cyclin D1 in non-small cell lung carcinoma and their clinical significance. *J Pathol*. 1999;188(4):351-360. doi:10.1002/(SICI)1096-9896(199908)188:4<351::AID-PATH385>3.0.CO;2-W

64. Xu H-J, Quinlan DC, Davidson AG, et al. Altered Retinoblastoma Protein Expression and Prognosis in Early-Stage Non-Small-Cell Lung Carcinoma. *JNCI J Natl Cancer Inst*. 1994;86(9):695-699. doi:10.1093/jnci/86.9.695

65. Ertel A, Dean JL, Rui H, et al. RB-pathway disruption in breast cancer. *Cell Cycle*. 2010;9(20):4153-4163. doi:10.4161/cc.9.20.13454

66. Taegtmeyer H, Sen S, Vela D. Return to the fetal gene program: a suggested metabolic link to gene expression in the heart. *Ann N Y Acad Sci*. 2010;1188:191-198. doi:10.1111/j.1749-6632.2009.05100.x

67. Lucien F, Brochu-Gaudreau K, Arsenault D, Harper K, Dubois CM. Hypoxia-induced invadopodia formation involves activation of NHE-1 by the p90 ribosomal S6 kinase (p90RSK). *PLoS One*. 2011;6(12):e28851. doi:10.1371/journal.pone.0028851

68. Muz B, de la Puente P, Azab F, Azab AK. The role of hypoxia in cancer progression, angiogenesis, metastasis, and resistance to therapy. *Hypoxia (Auckland, NZ)*. 2015;3:83-92. doi:10.2147/HP.S93413

69. Meng R. *Relative Quantification: Data Management & Analysis Settings*. www.bio-rad.com/genomics/pcrsupport. Accessed December 16, 2019.

70. Diss JKJ, Archer SN, Hirano J, Fraser SP, Djamgoz MBA. Expression profiles of voltage-gated Na+ channel ?-subunit genes in rat and human prostate cancer cell lines. *Prostate*. 2001;48(3):165-178. doi:10.1002/pros.1095

71. Laniado ME, Lalani EN, Fraser SP, et al. Expression and functional analysis of voltage-activated Na+ channels in human prostate cancer cell lines and their contribution to invasion in vitro. *Am J Pathol*. 1997;150(4):1213-1221. http://www.ncbi.nlm.nih.gov/pubmed/9094978. Accessed October 9, 2018.

72. Brisson L, Driffort V, Benoist L, et al. NaV1.5 Na+ channels allosterically regulate the NHE-1 exchanger and promote the activity of breast cancer cell invadopodia. *J Cell Sci*. 2013;126(21):4835-4842. doi:10.1242/jcs.123901

73. Sutoh Yoneyama M, Hatakeyama S, Habuchi T, et al. Vimentin intermediate filament and plectin provide a scaffold for invadopodia, facilitating cancer cell invasion and extravasation for metastasis. *Eur J Cell Biol*. 2014;93(4):157-169. doi:10.1016/j.ejcb.2014.03.002

74. Lanier MH, Kim T, Cooper JA. CARMIL2 is a novel molecular connection between vimentin and actin essential for cell migration and invadopodia formation. Bement W, ed. *Mol Biol Cell*. 2015;26(25):4577-4588. doi:10.1091/mbc.E15-08-0552

75. Kidd ME, Shumaker DK, Ridge KM. The role of vimentin intermediate filaments in the progression of lung cancer. *Am J Respir Cell Mol Biol*. 2014;50(1):1-6. doi:10.1165/rcmb.2013-0314TR

76. Gilles C, Polette M, Zahm JM, et al. Vimentin contributes to human mammary epithelial cell migration. *J Cell Sci*. 1999;112(24).

77. Besson P, Driffort V, Bon É, Gradek F, Chevalier S, Roger S. How do voltage-gated sodium channels enhance migration and invasiveness in cancer cells? *Biochim Biophys Acta - Biomembr*. 2015;1848(10):2493-2501. doi:10.1016/J.BBAMEM.2015.04.013

78. Tang Z, Scherer PE, Okamoto T, et al. Molecular cloning of caveolin-3, a novel member of the caveolin gene family expressed predominantly in muscle. *J Biol Chem*. 1996;271(4):2255-2261. doi:10.1074/jbc.271.4.2255

79. Kemp G, Young H, Fliegel L. Structure and function of the human Na^+/H^+ exchanger isoform 1. *Channels*. 2008;2(5):329-336. doi:10.4161/chan.2.5.6898

80. Ghovanloo M-R, Shuart NG, Mezeyova J, Dean RA, Ruben PC, Goodchild SJ. Inhibitory effects of cannabidiol on voltage-dependent sodium currents. *J Biol Chem*. 2018;293(43):16546-16558. doi:10.1074/jbc.RA118.004929

81. Narahashi T, Moore JW, Scott WR. Tetrodotoxin Blockage of Sodium Conductance Increase in Lobster Giant Axons. *J Gen Physiol*. 1964;47(5):965-974. doi:10.1085/JGP.47.5.965

82. Bean BP, Cohen CJ, Tsien RW. Lidocaine block of cardiac sodium channels. *J Gen Physiol*. 1983;81(5):613-642. doi:10.1085/jgp.81.5.613

83. Chahine M, Plante E, Kallen RG. Sea Anemone Toxin (ATX II) Modulation of Heart and Skeletal Muscle Sodium Channel α-Subunits Expressed in tsA201 Cells. *J Membr Biol*. 1996;152(1):39-48. doi:10.1007/s002329900083

84. McAllister SD, Soroceanu L, Desprez P-Y. The Antitumor Activity of Plant-Derived

Non-Psychoactive Cannabinoids. *J Neuroimmune Pharmacol*. 2015;10(2):255-267. doi:10.1007/s11481-015-9608-y

85. Fraguas-Sánchez AI, Fernández-Carballido A, Torres-Suárez AI. Phyto-, endo- and synthetic cannabinoids: promising chemotherapeutic agents in the treatment of breast and prostate carcinomas. *Expert Opin Investig Drugs*. 2016;25(11):1311-1323. doi:10.1080/13543784.2016.1236913

86. Ramer R, Hinz B. Cannabinoids as Anticancer Drugs. In: *Advances in Pharmacology (San Diego, Calif.)*. Vol 80. ; 2017:397-436. doi:10.1016/bs.apha.2017.04.002

87. Kim CH, Oh Y, Chung JM, Chung K. The changes in expression of three subtypes of TTX sensitive sodium channels in sensory neurons after spinal nerve ligation. *Mol Brain Res*. 2001;95(1-2):153-161. doi:10.1016/S0169-328X(01)00226-1

88. Fan Z, George AL, Kyle JW, Makielski JC. Two human paramyotonia congenita mutations have opposite effects on lidocaine block of Na+ channels expressed in a mammalian cell line. *J Physiol*. 1996;496(1):275-286. doi:10.1113/jphysiol.1996.sp021684

89. Cannon SC, Corey DP. Loss of Na+ channel inactivation by anemone toxin (ATX II) mimics the myotonic state in hyperkalaemic periodic paralysis. *J Physiol*. 1993;466(1):501-520. doi:10.1113/jphysiol.1993.sp019731

90. Nakajima T, Kubota N, Tsutsumi T, et al. Eicosapentaenoic acid inhibits voltage-gated sodium channels and invasiveness in prostate cancer cells. *Br J Pharmacol*. 2009;156(3):420-431. doi:10.1111/j.1476-5381.2008.00059.x

91. Padera RF, Tse JY, Bellas E, Kohane DS. Tetrodotoxin for prolonged local anesthesia with minimal myotoxicity. *Muscle Nerve*. 2006;34(6):747-753. doi:10.1002/mus.20618

92. Perez-Castro R, Patel S, Garavito-Aguilar Z V., et al. Cytotoxicity of Local Anesthetics in Human Neuronal Cells. *Anesth Analg*. 2009;108(3):997-1007. doi:10.1213/ane.0b013e31819385e1

93. Herceg Z, Ushijima T. *Epigenetics and Cancer. Part B*. Academic; 2010. https://books.google.ca/books?hl=en&lr=&id=8iyAM81U1cUC&oi=fnd&pg=PA237&dq=+Diet,+epigenetic,+and+cancer+prevention.&ots=LRQcRmfDaB&sig=d1JwygzVOChOMbDzfnw6kKyqr0k&redir_esc=y#v=onepage&q=Diet%2C epigenetic%2C and cancer prevention.&f=false. Accessed August 24, 2017.

94. Pal S, Tyler JK. Epigenetics and aging. *Sci Adv*. 2016;2(7):e1600584. doi:10.1126/sciadv.1600584

95. Esteller M. Epigenetics in Cancer. *N Engl J Med*. 2008;358(11):1148-1159. doi:10.1056/NEJMra072067

96. Sharma S, Kelly TK, Jones PA. Epigenetics in cancer. *Carcinogenesis*. 2010;31(1):27-36. doi:10.1093/carcin/bgp220

97. Berruti A, Bollito E, Cracco CM, et al. The prognostic role of immunohistochemical chromogranin a expression in prostate cancer patients is significantly modified by androgen-deprivation therapy. *Prostate*. 2010;70(7):n/a-n/a. doi:10.1002/pros.21104

98. Rashed MM, Bekele A. Neuroendocrine differentiation in a case of cervical cancer. *Pan Afr Med J*. 2010;6:4. http://www.ncbi.nlm.nih.gov/pubmed/21436947. Accessed October 18, 2018.

99. Makretsov N, Gilks CB, Coldman AJ, Hayes M, Huntsman D. Tissue microarray analysis of neuroendocrine differentiation and its prognostic significance in breast cancer. *Hum Pathol*. 2003;34(10):1001-1008. doi:10.1053/S0046-8177(03)00411-8

100. Papotti M, Macrì L, Finzi G, Capella C, Eusebi V, Bussolati G. Neuroendocrine differentiation in carcinomas of the breast: a study of 51 cases. *Semin Diagn Pathol*. 1989;6(2):174-188. http://www.ncbi.nlm.nih.gov/pubmed/2503862. Accessed October 12, 2018.

101. Weissferdt A, Moran CA. Neuroendocrine Differentiation in Thymic Carcinomas: A Diagnostic Pitfall. *Am J Clin Pathol*. 2016;145(3):393-400. doi:10.1093/ajcp/aqv095

102. Segawa Y, Takata S, Fujii M, et al. Immunohistochemical detection of neuroendocrine differentiation in non-small-cell lung cancer and its clinical implications. *J Cancer Res Clin Oncol*. 2009;135(8):1055-1059. doi:10.1007/s00432-009-0544-1

103. Khananshvili D. The SLC8 gene family of sodium–calcium exchangers (NCX) – Structure, function, and regulation in health and disease. *Mol Aspects Med*. 2013;34(2-3):220-235. doi:10.1016/J.MAM.2012.07.003

104. Pace CS, Tarvin JT. pH modulation of glucose-induced electrical activity in B-cells: Involvement of Na/H and HCO3/Cl antiporters. *J Membr Biol*. 1983;73(1):39-49. doi:10.1007/BF01870339

105. Turk E, Martin M, Wright E. Structure of the human Na+/glucose cotransporter gene SGLT1. http://www.jbc.org/content/269/21/15204.short. Accessed May 23, 2019.

106. McAinsh MR, Brownlee C, Hetherington AM. Calcium ions as second messengers in guard cell signal transduction. *Physiol Plant*. 1997;100(1):16-29. doi:10.1111/j.1399-3054.1997.tb03451.x

107. Berridge MJ, Bootman MD, Roderick HL. Calcium signalling: dynamics, homeostasis and remodelling. *Nat Rev Mol Cell Biol*. 2003;4(7):517-529.

doi:10.1038/nrm1155

108. Reid CA, Bekkers JM, Clements JD. Presynaptic Ca2+ channels: a functional patchwork. *Trends Neurosci*. 2003;26(12):683-687. doi:10.1016/J.TINS.2003.10.003

109. Rao VR, Perez-Neut M, Kaja S, Gentile S. Voltage-gated ion channels in cancer cell proliferation. *Cancers (Basel)*. 2015;7(2):849-875. doi:10.3390/cancers7020813

110. Phan NN, Wang C-Y, Chen C-F, Sun Z, Lai M-D, Lin Y-C. Voltage-gated calcium channels: Novel targets for cancer therapy. *Oncol Lett*. 2017;14(2):2059-2074. doi:10.3892/ol.2017.6457

111. Koliakos G, Paletas K, Kaloyianni M. NHE-1: A Molecular Target for Signalling and Cell Matrix Interactions. *Connect Tissue Res*. 2008;49(3-4):157-161. doi:10.1080/03008200802151581

112. Xiong J, Zhu MX. Regulation of lysosomal ion homeostasis by channels and transporters. *Sci China Life Sci*. 2016;59(8):777-791. doi:10.1007/s11427-016-5090-x

113. Lawrence SP, Bright NA, Luzio JP, Bowers K. The sodium/proton exchanger NHE8 regulates late endosomal morphology and function. *Mol Biol Cell*. 2010;21(20):3540-3551. doi:10.1091/mbc.E09-12-1053

114. Dolo V, D'Ascenzo S, Violini S, et al. Matrix-degrading proteinases are shed in membrane vesicles by ovarian cancer cells in vivo and in vitro. *Clin Exp Metastasis*. 1999;17(2):131-140. doi:10.1023/A:1006500406240

115. Becker A, Thakur BK, Weiss JM, Kim HS, Peinado H, Lyden D. Extracellular Vesicles in Cancer: Cell-to-Cell Mediators of Metastasis. *Cancer Cell*. 2016;30(6):836-848. doi:10.1016/J.CCELL.2016.10.009

116. Beghein E, Devriese D, Van Hoey E, Gettemans J. Cortactin and fascin-1 regulate extracellular vesicle release by controlling endosomal trafficking or invadopodia formation and function. *Sci Rep*. 2018;8(1):15606. doi:10.1038/s41598-018-33868-z

117. Angelucci A, D'Ascenzo S, Festuccia C, et al. Vesicle-associated urokinase plasminogen activator promotes invasion in prostate cancer cell lines. *Clin Exp Metastasis*. 2000;18(2):163-170. doi:10.1023/A:1006778000173

118. Ginestra A, La Placa MD, Saladino F, Cassarà D, Nagase H, Vittorelli ML. The amount and proteolytic content of vesicles shed by human cancer cell lines correlates with their in vitro invasiveness. *Anticancer Res*. 1998;18(5A):3433-3437. http://www.ncbi.nlm.nih.gov/pubmed/9858920. Accessed April 1, 2019.